The Limpopo magma-rich transform margin, South Mozambique – part 2: Implications for the Gondwana breakup

Vincent Roche, Sylvie Leroy, François Guillocheau, Sidonie Revillon, Gilles Ruffet, Louise Watremez, E. D'acremont, C. Nonn, W. Vetel, F. Despinois

Tectonics®

RESEARCH ARTICLE
10.1029/2021TC006914

The Limpopo Magma-Rich Transform Margin, South Mozambique – 2: Implications for the Gondwana Breakup

V. Roche[1], S. Leroy[1], F. Guillocheau[2], S. Revillon[3], G. Ruffet[2], L. Watremez[4], E. d'Acremont[1], C. Nonn[1], W. Vetel[5], and F. Despinois[5]

[1]Sorbonne Université, CNRS-INSU, Institut des Sciences de la Terre de Paris, Paris, France, [2]Université de Rennes, CNRS, Géosciences Rennes, Rennes, France, [3]SEDISOR/LGO UMR, Plouzané, France, [4]Université de Lille, CNRS, Université Littoral Côte d'Opale, IRD, UMR 8187—LOG—Laboratoire d'Océanologie et de Géosciences, Lille, France, [5]Totalenergies Exploration et Production, Pau, France

This article is companian to Watremez et al. (2021), https://doi.org/10.1029/2021TC006915

Key Points:

- A narrow ocean-continent transition characterizes the Limpopo magma-rich transform margin
- A set of major transform faults consistent with a dextral strike-slip system defines the Limpopo transform fault zone
- A long-lived magmatic activity marks the geodynamic evolution of Mozambique margins from early rifting to oceanic seafloor spreading

Supporting Information:

Supporting Information may be found in the online version of this article.

Correspondence to:

V. Roche,
vincent.roche@sorbonne-universite.fr

Citation:

Roche, V., Leroy, S., Guillocheau, F., Revillon, S., Ruffet, G., Watremez, L., et al. (2021). The Limpopo magma-rich transform margin, South Mozambique – 2: Implications for the Gondwana breakup. *Tectonics*, *40*, e2021TC006914. https://doi.org/10.1029/2021TC006914

Received 21 MAY 2021
Accepted 21 OCT 2021

Abstract The rifted continental margins of Mozambique provide excellent examples of continental passive margins with a significant structural variability associated with magmatism and inheritance. Despite accumulated knowledge, the tectonic structure and nature of the crust beneath the South Mozambique Coastal Plain (SMCP) are still poorly known. This study interprets high-resolution seismic reflection data paired with data from industry-drilled wells and proposes a structural model of the Limpopo transform margin in a magma-rich context. Results indicate that the Limpopo transform margin is characterized by an ocean-continent transition that links the Beira-High and Natal valley margin segments and represents the western limit of the continental crust, separating continental volcano-sedimentary infilled grabens from the oceanic crust domain. These basins result from the emplacement of the Karoo Supergroup during a Permo-Triassic tectonic event, followed by an Early Jurassic tectonic and magmatic event. This latter led to the establishment of steady-state seafloor spreading at ca.156 Ma along the SMCP. A Late Jurassic to Early Cretaceous event corresponds to formation of the Limpopo transform fault zone. Which accommodated the SSE-ward displacement of Antarctica with respect to Africa. We define a new type of margin: the magma-rich transform margin, characterized by the presence of voluminous magmatic extrusion and intrusion coincident with the formation and evolution of the transform margin. The Limpopo transform fault zone consists of several syn-transfer and -transform faults rather than a single transform fault. The intense magmatic activity was associated primarily with mantle dynamics, which controlled the large-scale differential subsidence along the transform margin.

1. Introduction

Divergent-transform continental margins represent about 30% of Earth's continental margins (Mercier de Lepinay et al., 2016), but they have only been sparsely studied (e.g., Basile, 2015; Nemčok et al., 2016), especially in comparison with the other divergent types (i.e., normal or oblique). As a result of first-order plate separation processes, transform continental margins develop in three main phases (e.g., Bird, 2001; Lorenzo, 1997; Mascle & Blarez, 1987), starting with the rift stage in which a continental lithospheric shear zone may develop, followed by the onset of seafloor spreading at a neighboring thinned divergent margin segment, and ending with an oceanic spreading stage where the oceanic crust slides along the continental crust of the transform margin. According to Basile (2015), the duration of each stage increases from one extremity to the other. The intersection between transform margin and divergent margin are named the inner corner at the beginning of the transform margin–that is – toward the continent, and the outer corner at its opposite side–that is – toward the oceanic spreading axis.

Transform margins are generally defined (e.g., Basile et al., 1993; Francheteau & Le Pichon, 1972; Mascle, 1976; Loncke et al., 2019; Mercier de Lepinay et al., 2016; Nemčok et al., 2016; Sage et al., 2000) by (a) an unequivocal continental crust, sharply thinned in distal parts of the margins, defining a narrow necking zone ranging generally from 50 to 100 km wide, (b) steep continental slopes, (b) occasionally marginal ridges located at the edge of the continental slope, (c) marginal plateaus systematically located between the platform and the lower continental slope, and (d) some specific sedimentary processes (e.g., slope instabilities). Thus, they show a large variability of vertical displacements that result from their length and their long-lived evolution. Nonetheless, these morpho-tectonic units are not systematic, suggesting that key parameters such as pre-existing lithospheric heterogeneities and related thermal state, fluids (e.g., dewatering and/or hydrothermalism) and magmatic activity may strongly

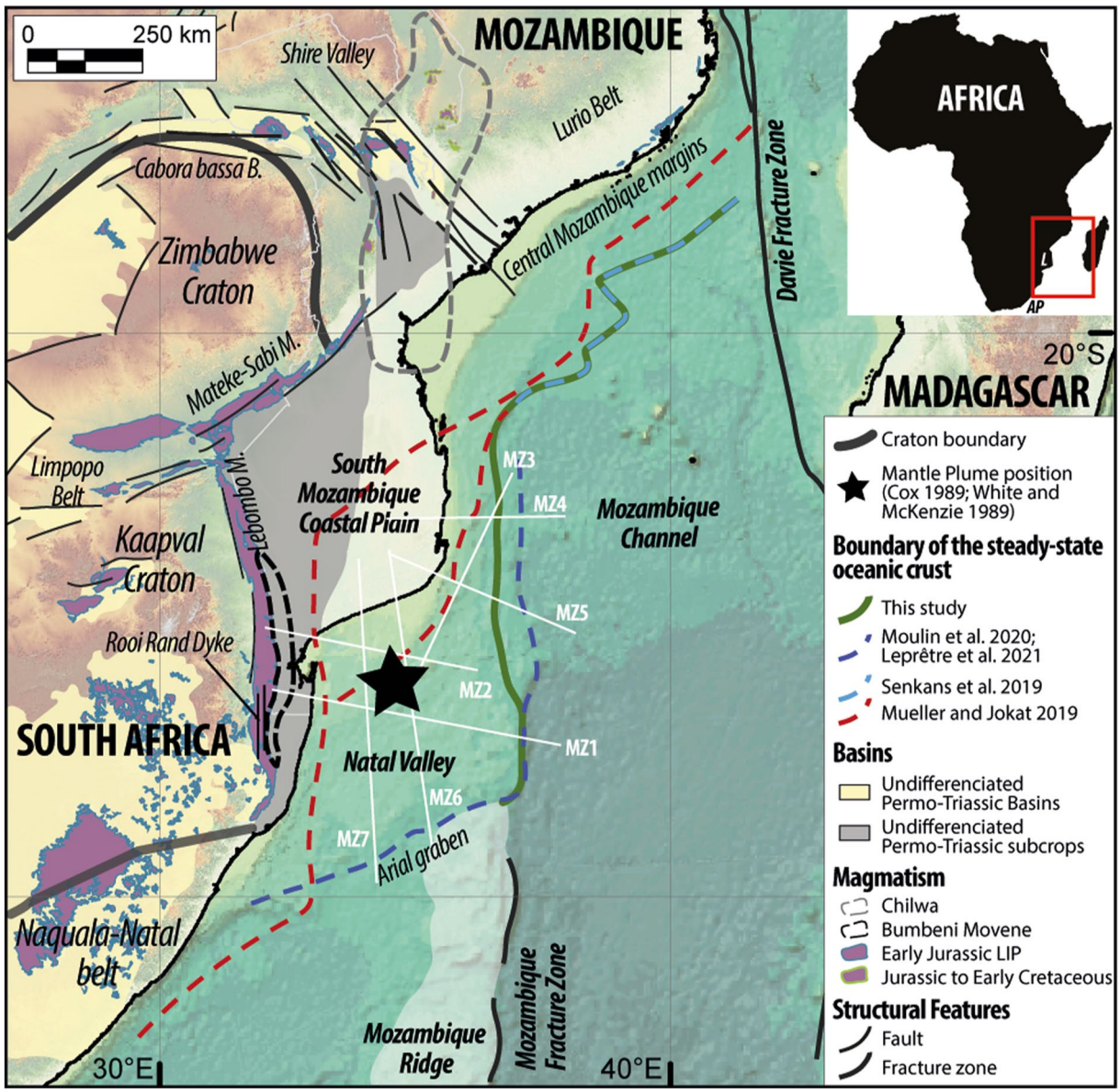

Figure 1. Map of the study area located in the southeastern part of Africa plate. Note the onshore location of the main Permo-Triassic basins and faults according to Daszinnies et al. (2009). White lines correspond to the location of seismic refraction profiles from PAMELA-MOZ3/5 experiment (Moulin & Aslanian, 2016; Moulin & Evain, 2016) (see text for more information). MZ4 and MZ5 are presented in the companion paper from Watremez et al. (2021). Red box in the top right corner shows the location of the study area. AP (Agulhas Plateau), B (Basin), L (Limpopo).

influence their formation as described in various studies of divergent margins (e.g., Clerc et al., 2018; Ebinger & Casey, 2001; Lucazeau et al., 2010; Manatschal, 2004).

In this study, we investigate the extension of the Mozambique Ridge (MR) in the Limpopo area (e.g., Fischer et al., 2016; König & Jokat, 2010), which is located east of Africa between 28°S and 36°S of longitude within the western part of the oceanic Mozambique Basin along the Natal Valley (Figure 1). Here, recent seismic refraction models suggest the presence of continental crust below the South Mozambique Coastal Plain (SMCP) which extends southward toward the Natal Valley (Leprêtre et al., 2021; Moulin et al., 2020) and brings into question most of the paleo-reconstructions of the Gondwana (e.g., Eagles & König, 2008; Gaina et al., 2013; Leinweber & Jokat, 2012). This implies that the continent-ocean boundary may extend as far south as the north end of the MR where the oceanic crust has been mapped in previous studies (e.g., Hanyu et al., 2017; Raillard, 1990).

Our interpretation of seismic reflection data and $^{39}Ar/^{40}Ar$ ages of volcanic rocks from one well (Funhalouro well located in the SMCP, Figure 1) provide new constraints on the structure and nature of the crust and on the development of the Limpopo continental transform margin between Africa and Antarctica. This study complements the study of Senkans et al. (2019) along the Central Mozambique margins. We also propose that the Limpopo margin may be considered a magma-rich transform margin.

2. Geological Setting

2.1. Southeastern Africa: Tectonic and Magmatic Features

Geology of southeastern Africa consists of Archean and Paleoproterozoic cratonic masses (i.e., the Kaapval and Zimbabwe cratons) surrounded by Mesoproterozoic and Neoproterozioc orogenic belts mainly accreted during several Precambrian orogenic events (e.g., Cawood & Buchan, 2007; Collins & Pisarevsky, 2005; Jacobs & Thomas, 2004; Ring et al., 2002). Such continental block amalgamation favored the formation of crustal-scale structures with two main regional trends which were reactivated during the Phanerozoic (e.g., Castaing, 1991; Daly et al., 1989; Macgregor, 2018). The first regional trend, roughly parallel to the coastline, is oriented NE-SW and extends along the Matake-Sabi Monocline (Figure 1). It corresponds primarily to the regional ductile fabric trend of the metamorphic basement of the Lurio and the Limpopo orogenic belts (Daszinnies et al., 2009). The second structural trend is approximately NW-SE trending and is mainly marked by the Shire valley at the edge of the Lurio belt (Figure 1) (Castaing, 1991), becoming N-S along the southern part of the Lebombo Monocline. Interestingly, both trends were reactivated locally during (a) the Permian-Triassic time as evidenced by the presence of Karoo rifts associated with the Karoo Supergroup (e.g., Castaing, 1991; Catuneanu et al., 2005; Galasso et al., 2019; Watkeys, 2002) and (b) the Early to Middle Jurassic (e.g., Cox, 1992; Castaing, 1991) as evidenced by the presence of a large igneous province (LIP) and various set of faults which locally controlled the LIP emplacement (ca. 180 Ma, Duncan et al., 1997; Riley et al., 2004; Jourdan et al., 2007; Svensen et al., 2012). Unfortunately, the SMCP basin which consists of Cretaceous to Quaternary primarily siliciclastic sediments (Baby et al., 2018; Salman & Abdula, 1995), may partially obscure these deposits and structures.

The continental rifting between Africa (Mozambique) and Antarctica (Dronning Maud Land) is thought to have begun ~180 Ma ago (e.g., Cox, 1992; Mahanjane, 2012; Reeves, 2017), contemporaneous with the LIP which crops out around the SMCP (Lebombo and Mateke-Sabi Monoclines, Figure 1; e.g., Klausen, 2009; Melluso et al., 2008) and in Antarctica (i.e., the Ferrar Igneous Province, Encarnacion et al., 1996) reaching a thickness of 12 km locally (Riley et al., 2004). It has been proposed that this widespread magmatic activity is related to the plume emplacement (Storey & Kyle, 1997; White & McKenzie, 1989; White, 1997). The age of breakup along the Mozambique margin is a matter of debate, ranging from chron 38n (ca. 166 Ma) to chron 33n (ca. 161 Ma) along the Angoche segment to chron 25n along the Beira High segment (ca. 156 Ma) (Figure 1; ;Leinweber & Jokat, 2012; Leinweber et al., 2013; Mueller and Jokat, 2017, 2019; Senkans et al., 2019). Consequently, the youngest post-rift sediments on the margins and the oldest sediments on the oceanic crust are estimated to be of Middle to Late Jurassic age depending on the segment. Interpretation of the magnetic anomalies indicates that kinematic movement of this region is thought to have rotated progressively from NW-SE to a N-S orientation during the Late Jurassic (e.g., Cox, 1992; Klimke et al., 2018; Nguyen et al., 2016; Reeves, 2017; Senkans et al., 2019), resulting in the rapid onset of seafloor spreading along the SMCP at around 156 Ma (Figure 2). In addition, these displacements were accompanied by widespread volcanism in southern Africa beginning at 185 Ma (i.e., LIP emplacement). Emplacement of two later magmatic provinces occurred during the uppermost Jurassic to Early Cretaceous: the Bumbeni-Movene magmatic province (145–131 Ma, e.g., Cleverly & Bristow, 1979; Watkeys, 2002) in the southern part of the Lebombo and the Chilwa magmatic province (133–105 Ma, e.g., Castaing, 1991; Flores, 1984; Woolley, 1991) primarily in the northern part of the SMCP (Figure 1).

2.2. The South Mozambique Coastal Plain and the Natal Valley: Main Controversies

The nature of the crust onshore in the SMCP and the Natal Valley has been discussed for decades in attempts to resolve issues surrounding various plate reconstruction models. Several of these models suggest that Antarctica overlapped the SMCP, implying the presence of oceanic crust below this area and the Natal Valley (e.g., Eagles & König, 2008; Gaina et al., 2013; Jacobs & Thomas, 2004; Jokat et al., 2003; König & Jokat, 2006; Leinweber & Jokat, 2012; Nguyen et al., 2016; Reeves et al., 2016; Reeves, 2017; Seton et al., 2012). However, recent

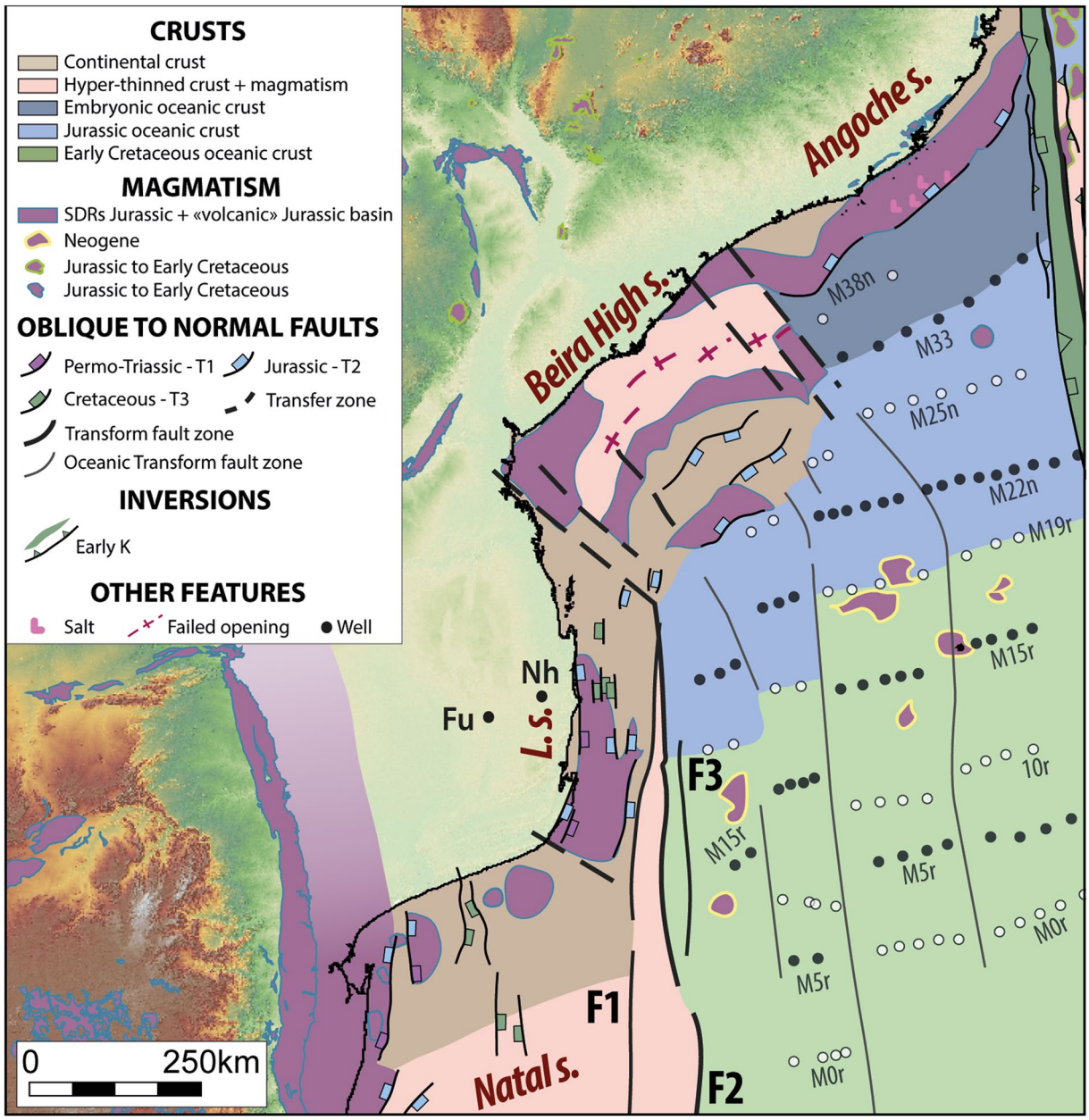

Figure 2. Structural map for the Central Mozambique margin based on our observations and modified after Senkans et al. (2019). Note that Jurassic faults along the Beira-High and Angoche are from Senkans et al. (2019). The map shows a segmentation of the Mozambique margins with, from west to east the Natal, Limpopo, the Beira High and Angoche segments. Magnetic anomaly identifications are after Mueller and Jokat (2019). T_1, T_2, and T_3 (see discussion) correspond to the three main stages, see text for details. L (Limpopo), F (Fault), Fu (Funhalouro), Na (Nhachengue), s (Segments).

reconstruction models of the Indian Ocean (Thompson et al., 2019) suggests that the SMCP is continental in origin, in agreement with the first plate kinematic analysis of the Mozambique Basin (Raillard, 1990; Segoufin & Patriat, 1981). Recent seismic studies using P-waves velocity models established on seven refraction profiles acquired aboard the R/V Pourquoi Pas? During the PAMELA-MOZ3-5 cruise, support the interpretation of the Mozambique Basin as continental in origin (Moulin & Aslanian, 2016; Moulin & Evain, 2016; Moulin et al., 2020; Leprêtre et al., 2021; Watremez et al., 2021). Moulin et al. (2020) and Leprêtre et al. (2021) identified two crustal domains. The first one is located on the SMCP and ends in the North Natal Valley (around 29°S) and corresponds to the continental domain, possibly with magmatic intrusions. Here, the crust reaches 35–40 km in thickness and thins eastward by crustal necking from 35°E to 37°E (Figure 2). The second one, located southward and

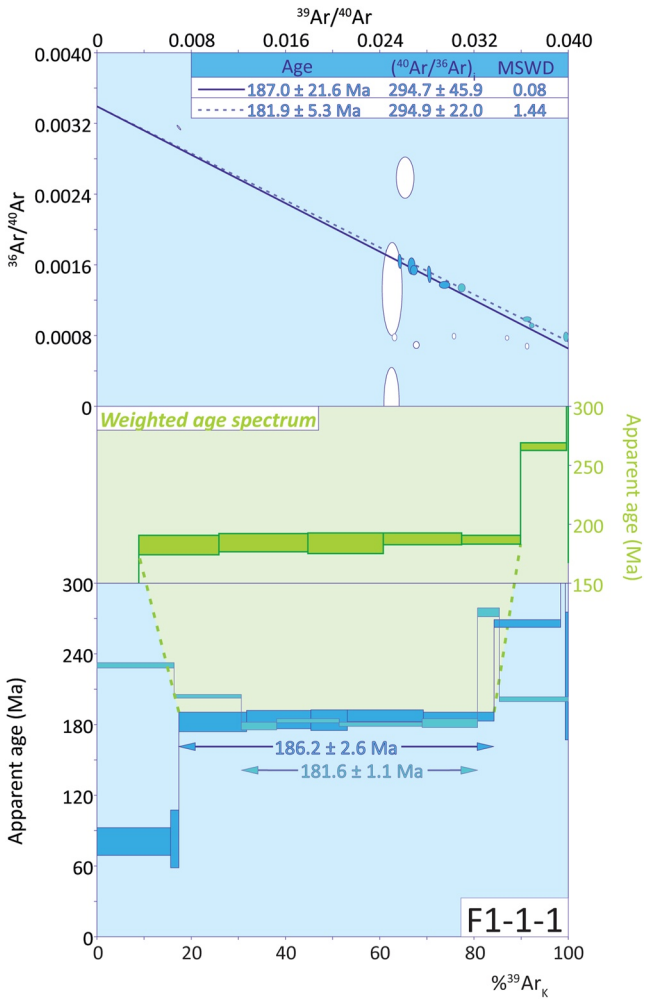

Figure 3. ^{40}Ar-^{39}Ar step-heating age spectra of two whole rock fragments from the Funhalouro well. Integrated ages are given with 1σ. Sample locations are indicated in Figure 2. Analytic data are indicated in the Supporting Information (see Tables S1, S2 and S3 in Supporting Information S1).

eastward, is the oceanic domain that corresponds well with the location of the identified magnetic anomalies in the Mozambique Basin (Figure 2; Mueller & Jokat, 2019). These interpretation of the nature of the crust are consistent with the recent study of Li et al. (2021) using one seismic reflection profile located in the Natal Valley.

The origin and nature the Limpopo area, extending southward along the Mozambique Fracture Zone (F.Z.) and the MR remains enigmatic due to the lack of seismic reflection data and well calibrations. Some studies suggest it is underlain by continental crust based on refraction data (Tucholke et al., 1981; Moulin et al., 2020; Leprêtre et al., 2021; Watremez et al., 2021), reflection data (Li et al., 2021; Raillard, 1990), gravity data (Hanyu et al., 2017) and dredge sample analyses (Mougenot et al., 1991; Raillard, 1990). Others proposed it to be a microcontinental fragment embedded in oceanic crust (Ben-Avraham et al., 1995; Reeves, 2017; Reeves et al., 2016) or favor an oceanic origin based on magnetic and gravity anomalies (König & Jokat, 2010). Based on the geometric relationships between magnetic anomalies and magma emplacement, a Lower Cretaceous age is proposed for the volcanic activity along the MR (between 140 Ma to 122 Ma, Gohl et al., 2011 and/or ∼131 and ∼125 Ma, Fischer et al., 2016).

3. Instruments and Methods

3.1. Data

We used seismic reflection data provided by TOTALENERGIES, together with refraction profiles from the PAMELA-MOZ3/5 cruise aboard the R/V Pourquoi Pas? (Moulin & Aslanian, 2016; Moulin & Evain, 2016). Our data set consists primarily of an extensive set of onshore and offshore 2D seismic reflection profiles and three wells (two wells located in the SMCP, Figure 1 and one well located in the Zambezi Basin, see Ponte et al. (2019)), which have been used to constrain our interpretation of lithology and age in the seismic data (see Figure 3). Note that the two wells are located on onshore seismic lines (see the blue dotted line, Figure 4) and cannot be shown for reasons of proprietary confidentiality. The key stratigraphic layers from these wells were readily extended along the five offshore seismic profiles. The depth-time conversion of the seismic refraction data of the study of Watremez et al. (2021) makes possible to trace these dated surfaces in the seismic section. These surfaces were then identified along seismic lines as belonging to the same reflector.

In this study we present the five most useful offshore WesternGeco seismic profiles. Four profiles trend E-W to WNW-ESE, that is, roughly perpendicular to the present-day coastline (Figures 4–7 and location herein). These profiles are thus perpendicular to the oceanic seafloor spreading direction. The profile at the distal part of the margin trends N-S (Figure 8). Note that this profile is close to the location of the identified magnetic anomalies (Mueller & Jokat, 2019). All seismic profiles have a maximum penetration depth of up to 10 s TWTT and seismic sections were interpreted using considerable vertical exaggeration (e.g., Figure 4). The quality of the seismic lines in some places reveal sedimentary sequences, the basement and the deep crustal structures in places, the interpreted oceanic Moho and occasionally intra-mantle reflections may also be seen. We recognized three crustal domains, which are consistent with the study of Watremez et al. (2021). The first one is located below the coastal plain and corresponds to the continental domain (P-wave velocities of 5.5 to >7 km/s) and the crust thicknesses onshore range from 30 to 32 km (Watremez et al., 2021). The second one represents the transitional domain with a western zone that may correspond to the uppermost continental crust intruded by magmatism and an eastern zone that appears to be over-thickened oceanic crust indicative of greater magma supply (Watremez et al., 2021).

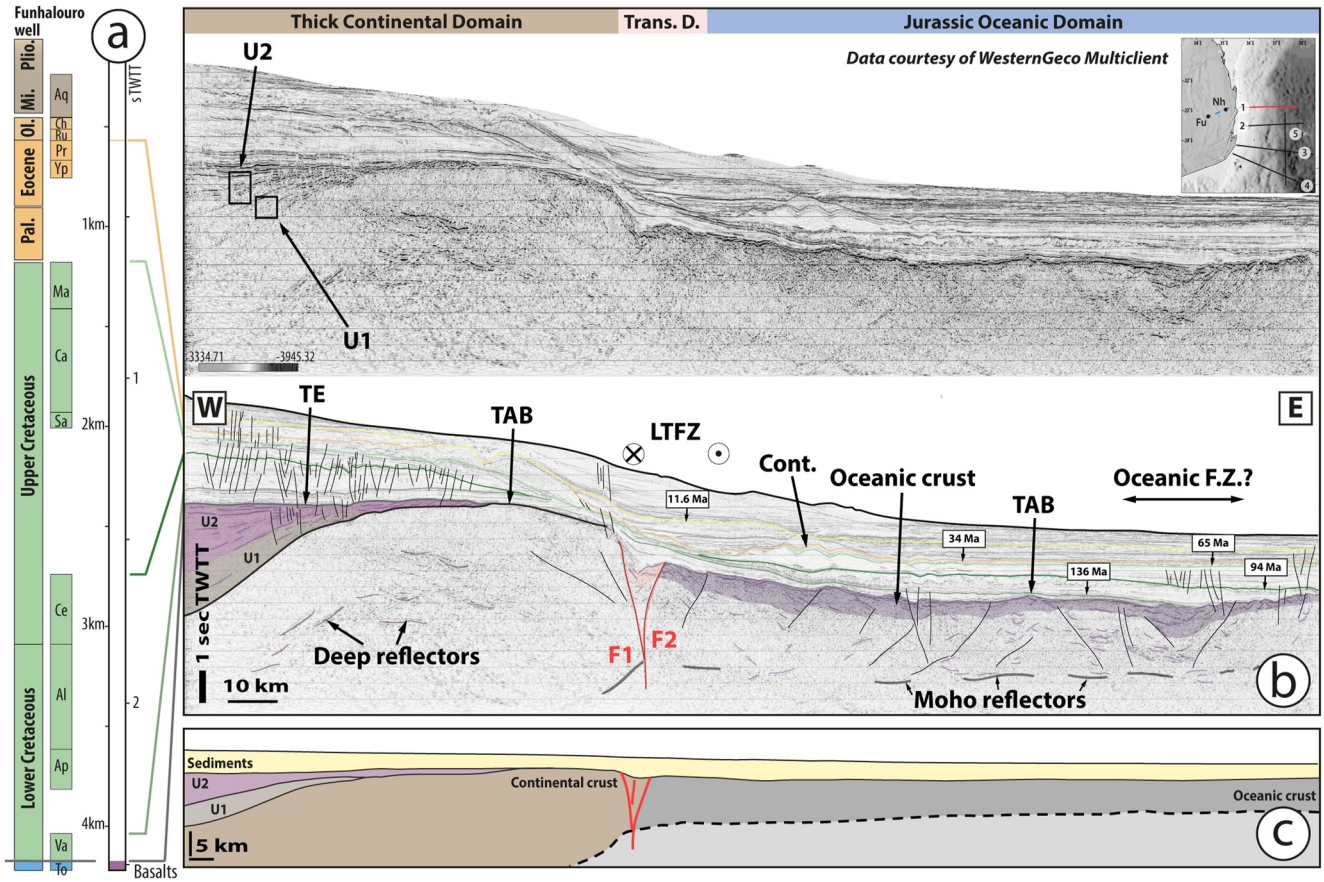

Figure 4. (a) Funhalouro well showing the main horizons used to calibrate our seismic lines. Note the presence of volcanic rocks at the bottom of the well dated at 180.3 ± 0.8 Ma and 178.9 ± 1.4 Ma through the argon method. These rocks correspond to the top of U2 unit. Series Epoch: Plio, Pliocene; Mi, Miocene; Ol, Oligocene; Pal; Paleocene. Stage Age: Aq, Aquitanian; Ch, Chattian; Ru, Ruppelian; Pr, Priabonian; Yp, Ypresian; Ma, Maastrichian; Ca, Campanian; Sa, Santonian; Ce, Cenomanian; Al, Albian; Ap, Aptian; Va, Valanginian; To, Toarcian. (b) E-W trending offshore seismic profile #1 with line drawing and interpretation of the sediment and basement structures observed. The distinct domains are identified above the seismic profile. Note also that violet color corresponds to the upper part of oceanic crust for all transects. Note that the red line in the inset corresponds to the profile location shown in this figure whereas the blue dotted line indicates the position of onshore seismic lines (not shown for confidentiality reasons) used to extend well calibration. See text for explanations. Cont., Contourites; F, Fault; F.Z., Fracture Zone; LTFZ, Limpopo Transform Fault Zone; TAB, Top Acoustic Basement; TE, Top Erosional surface; Trans. D., Transitional Domain. (c) Simplified interpretation of the seismic profile converted in km-depth and drawn with no vertical exaggeration.

The last domain is characterized by an 8–9 km to 9–13 km-thick oceanic crust from north to south (Watremez et al., 2021), respectively.

3.2. Seismic Stratigraphy

Although a detailed study of the sedimentary succession is beyond the scope of this paper, Baby et al. (2018) and Ponte et al. (2019) interpreted four key stratigraphic layers as having been deposited during the post-rift interval. This is consistent with other findings in the literature on the South Mozambique Coastal Plain (e.g., Salman & Abdula, 1995; Mahanjane, 2012, 2014; Klimke et al., 2018). From oldest to youngest, they correspond to (a) the uppermost Valanginian, (b) the top Cenomanian, (c) the top Cretaceous, (d) the top Eocene. Here, this post-rift unit starts with thin continental sandy red beds (mostly barren of pollen and microfossils and except for some fossils of Valanginian age, Baby et al., 2018), overlying weathered volcanic rocks tentatively attributed to the Early Jurassic (Flores, 1984; Raillard, 1990; Salman & Abdula, 1995).

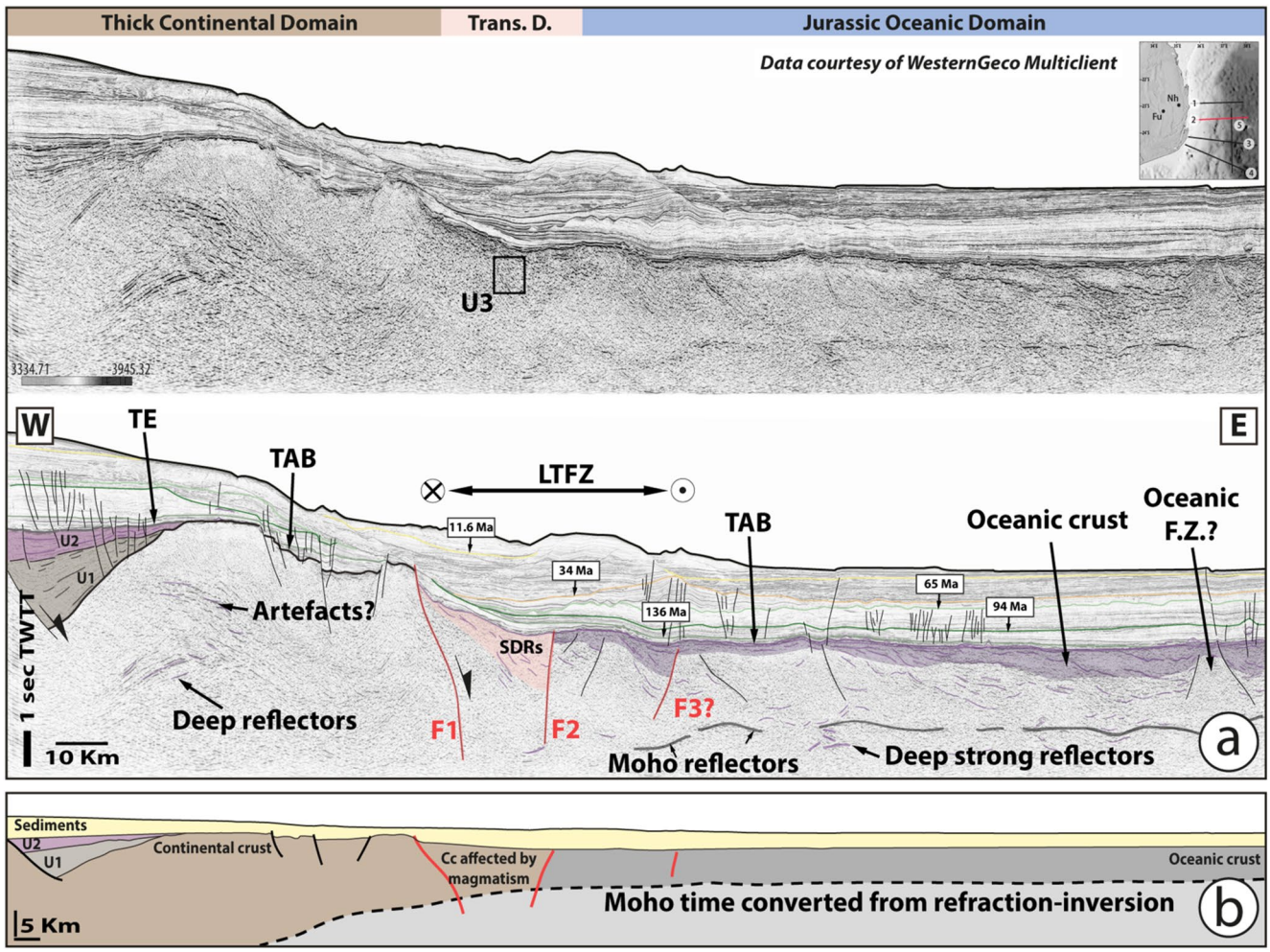

Figure 5. (a) Seismic profile #2 with our interpretation. The distinct domains identified are indicated above the seismic profile. Note also the presence of strong reflectors below the Moho within the oceanic domain. See inset for profile location. See text for explanations. F, Fault; F.Z., Fracture Zone; LTFZ, Limpopo Transform Fault Zone; OSDRs, Oceanic Seawards Dipping Reflectors; SDRs, Seaward Dipping Reflectors; TAB, Top Acoustic Basement; TE, Top Erosional surface; Trans. D., Transitional Domain. (b) Simplified interpretation of the seismic profile converted in km-depth and drawn with no vertical exaggeration. Cc, Continental Crust.

3.3. $^{40}Ar/^{39}Ar$ Sampling in Funhalouro Well

In order to confirm the Early Jurassic age of the volcanic rock plugs collected from the bottom of Funhalouro, we used the $^{40}Ar/^{39}Ar$ method (Figure 2; see Text S1 in Supporting Information S1). Here, sample (F1-1-1 plug from Funhalouro well cores) corresponds to a reworked rhyolitic tuff sampled at ca. 4,217 meters depth.

4. Results and Interpretations

4.1. $^{40}Ar/^{39}Ar$ Results

The $^{40}Ar/^{39}Ar$ analyses of two plugs of F1-1-1 (Figure 2) provide distinct age spectra (Figure 3), staircase-shaped or saddle-shaped, a disparity that could be attributed to the very strong heterogeneity of analyzed material and the probable occurrence of inherited components. Nevertheless, in intermediate temperature steps, these two age spectra converge along flat segments that produced ages that are broadly consistent with those of the pseudo-plateau, 186.2 ± 2.6 Ma (66.9% of the total $^{39}Ar_K$ released) and 181.6 ± 1.1 Ma (50.1% of the total $^{39}Ar_K$ released). The isochron calculations ($^{36}Ar/^{40}Ar$ vs. $^{39}Ar_K/^{40}Ar^*$; Turner, 1971; Roddick et al., 1980; Hanes et al., 1985) carried out on these segments, with $(^{40}Ar/^{39}Ar)_i$ ratios in compliance with atmospheric ratio, do not reveal any particular anomaly. The weighting process (De Putter et al., 2015; De Putter & Ruffet, 2020; Tremblay et al., 2020) of the staircase-shaped age spectrum results in an increase of c. 21% of the segment of interest, to represent c.

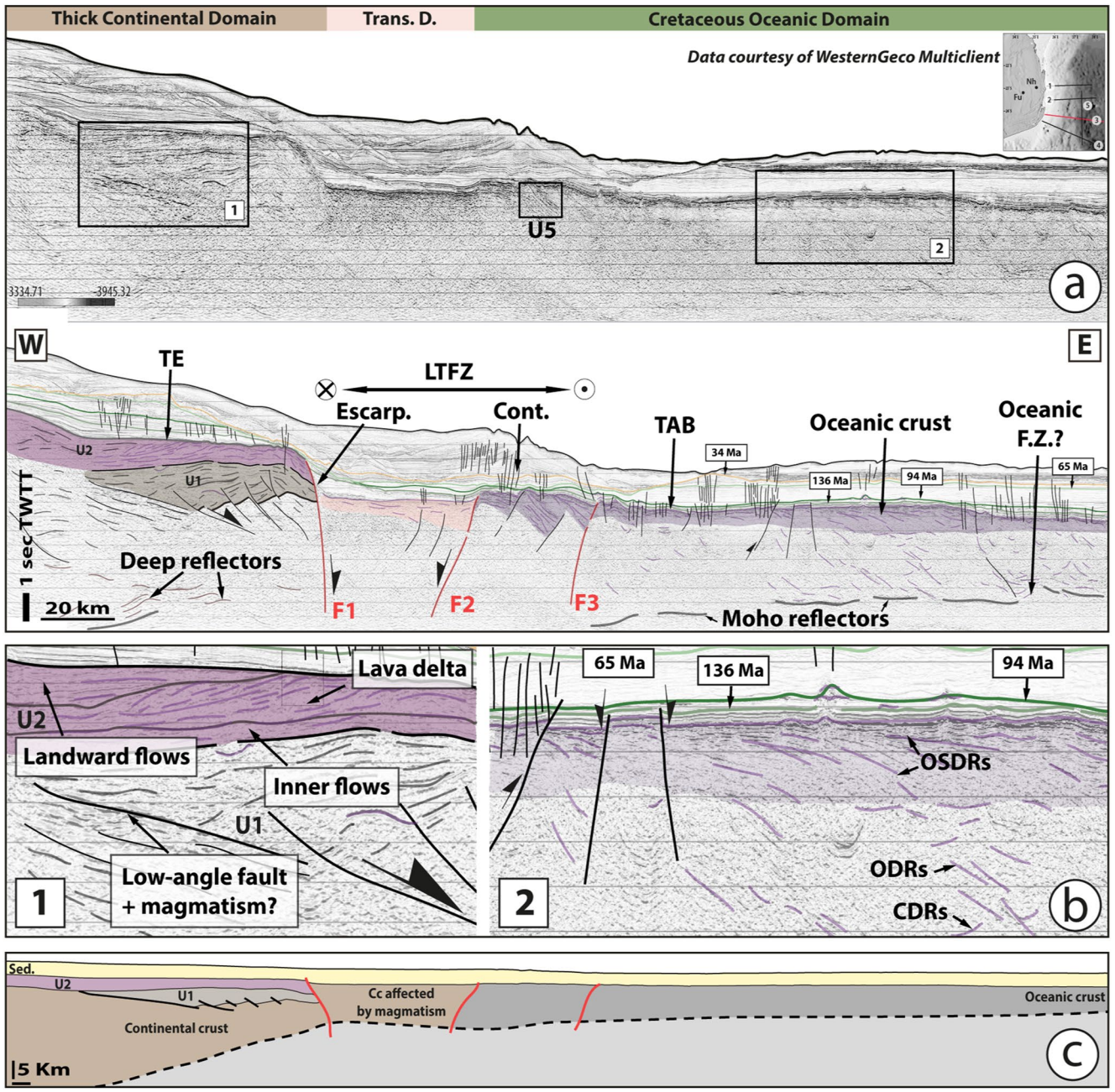

Figure 6. E-W offshore profiles #3 showing line drawing and interpretation of the sediment and basement structures observed. The distinct domains are identified above the seismic profile. See inset for profile location. Escarp, Escarpment; Cont, Contourites; F, Fault; F.Z., Fracture Zone; LTFZ, Limpopo Transform Fault Zone; TAB, Top Acoustic Basement; TE, Top Erosional surface; Trans. D., Transitional Domain. (b) Zoom showing the internal structures. See text for explanations. (c) Simplified interpretation of the seismic profile converted in km-depth and drawn with no vertical exaggeration. Cc, Continental Crust.

81% of the resulting weighted age spectrum, suggesting that the associated radiogenic component is the principal component of the analyzed whole rock fragment. This suggests that the F1-1-1 rhyolitic tuff may be early Jurassic in age (Figure 3). Consequently, Funhalouro well provides a good constraint on markers and seismic facies down to Lower Jurassic in the SMCP. In our interpretation, this dated surface corresponds to the TE horizon in the offshore seismic profiles (Figures 4–7). We describe these facies in detail below (see Section 4.2).

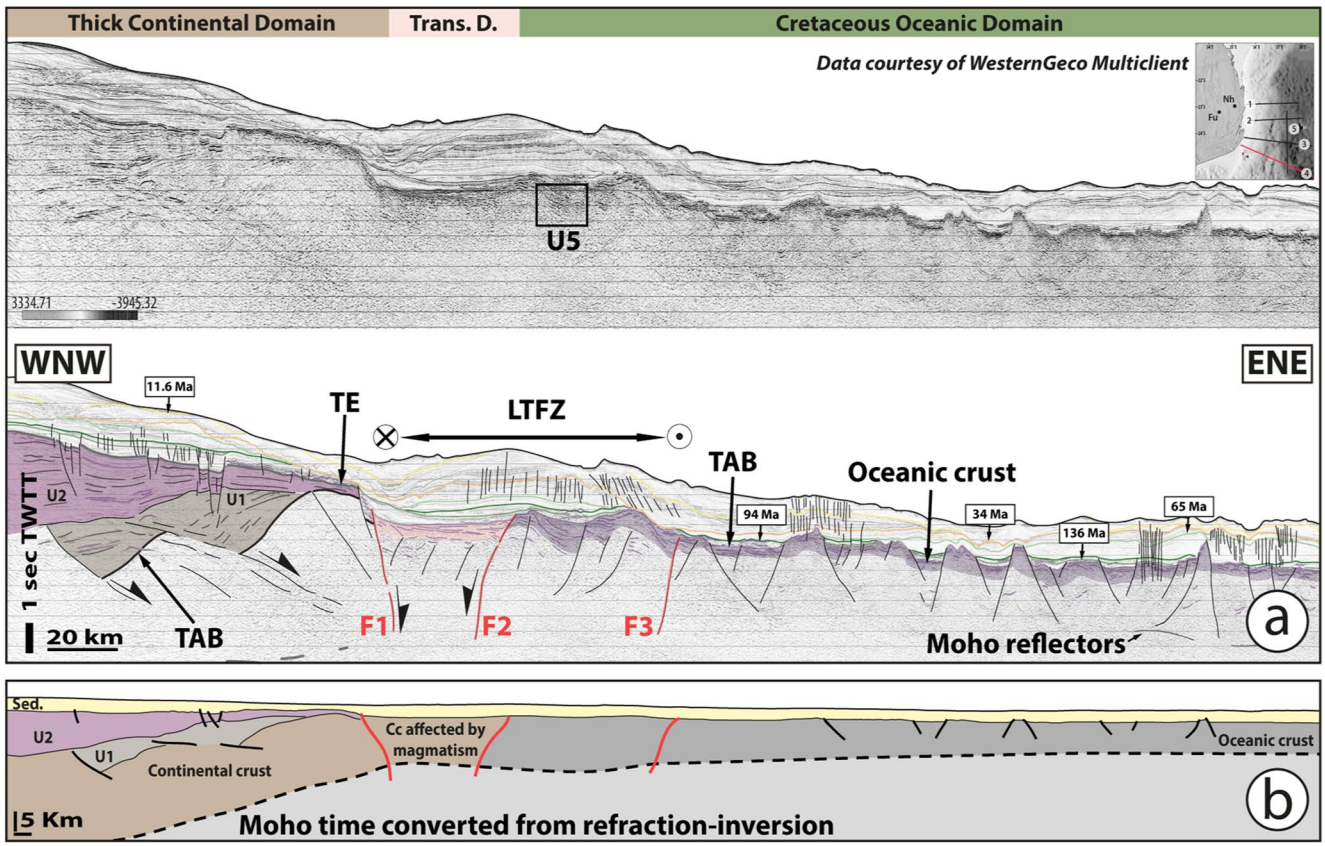

Figure 7. (a) E-W offshore profile #4 showing line drawing and interpretation of the sediment and basement structures observed. The distinct domains identified are indicated above the seismic profile. See inset for profile location. See text for explanations. F, Fault; LTFZ, Limpopo Transform Fault Zone; TAB, Top Acoustic Basement; TE, Top Erosional surface, Trans. D., Transitional Domain. (b) Simplified interpretation of the seismic profile converted in km-depth and drawn with no vertical exaggeration.

4.2. Crustal Domains: Principal Seismic Facies Observations From Seismic Profiles

4.2.1. The Continental Domain

Two principal seismic units (U1 and U2) are recognized in the western part of profiles before the major escarpment (Figures 4–7). U1 is characterized by a set of transparent to low amplitude parallel reflectors (Figure 4 and Table 1), showing fault-bounded wedge-shaped geometries with eastward onlaps onto basement high and ranging from 1 to 2.5 s TWTT in thickness toward the west along the faults depending on the area (Figures 4 and 7). We suggest that U1 is primarily made up of sediments but magmatic addition cannot be totally excluded (see sills in Figure 7). Above this underlying seismic unit, another set of reflectors can be identified. It is seismically characterized by a set of 5–15 km-long reflectors, showing also fault-bounded wedge-shaped geometries (Figures 4, 5, and 7). These bright and coherent reflectors have strong amplitudes and low to medium frequency and belong to U2 (Figure 4 and Table 1). In addition, U1 reflectors are cut locally by U2 reflectors (Figure 7) implying that the contact between U1 and U2 is disconformable. Further, sample F1-1-1 was collected at the top of U2, indicating a volcanic origin for these reflectors (Figure 4a). This is in good agreement with the seismic characteristics of the reflectors (e.g., Planke et al., 2000) suggesting large lava flows and/or interstratified volcanoclastics and lava flows. In addition, along Profile #3 (Figure 6b), U2 results from the stacking of three seismic subunits that may be interpreted as lava delta. From base to top, the first subunit is made up of quasi-horizontal and quasi-continuous bright reflectors that are almost parallel to the top of the U1, the second subunit is composed of landward prograding clinoforms (strong amplitudes and medium frequency reflectors), the last subunit consists of flat horizontal reflectors (0.25 s TWTT thick), sub-parallel to the overlying major erosional contact described at the end of this section. Such infilling geometry looks similar to the succession described by Abdelmalak et al. (2016) for the Vøring escarpment in Norway, and thus may locally correspond to lava delta systems with both landward

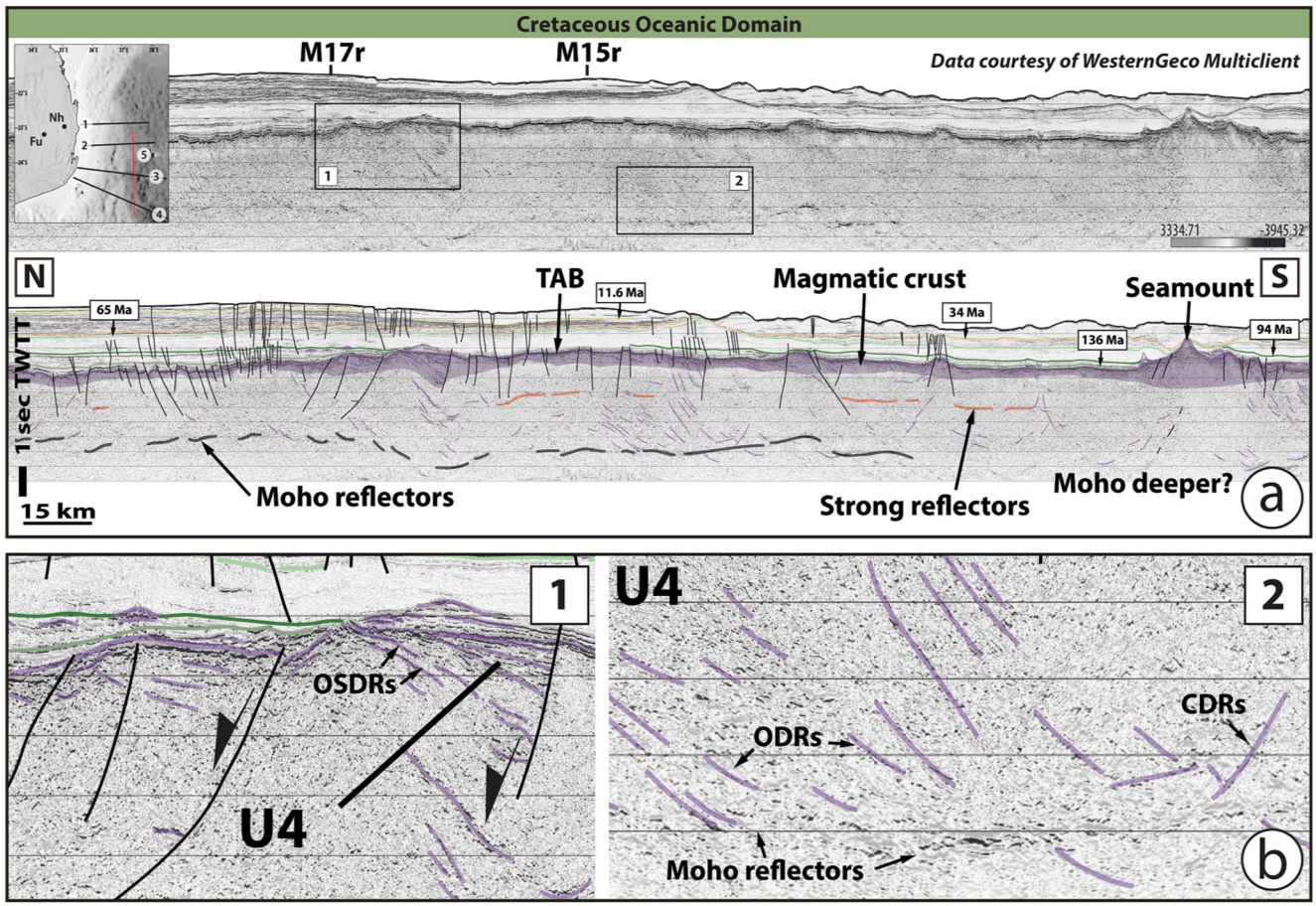

Figure 8. (a) N-S offshore seismic profile #5 located in the oceanic domain with line drawing and interpretation of the sedimentary sequence and the basement structures observed. Magnetic anomaly identification is after Mueller and Jokat (2019). Note that the chron is slightly shifted southwest to be positioned on the seismic profile. See inset for profile location. (b) Close-up views showing the detailed seismic structures below TAB (Top Acoustic Basement). See text for explanations. CDRs, Continentward Dipping Reflectors; OSDRs, Oceanic Seawards Dipping Reflectors; ODRs, Oceanward Dipping Reflectors.

(subaerial or shallow marine flood basalts) and inner lava (shallow marine deposited) flows at its top and its base respectively (subset 1, Figure 6). Thus, U2 may be made up of a volcano-sedimentary and/or only volcanic rocks. Interestingly, the top of this unit is defined by an erosional surface (TE horizon) (e.g., Figure 7), cutting through U2. The presence of thin Valanginian continental sandy red beds (lacustrine to alluvial) far from the shoreline above U2 highlights the uplift of the western part of the margin occurring before the post-rift sediments deposition.

Another seismic unit (U3) is recognized below the top acoustic basement (TAB), east of the foot of the major escarpment (e.g., Figure 6). This unit extends eastwards, up to 40 km away from the escarpment (Figure 7). This specific unit shows no clear geometric relation to the previous ones and therefore its position in the chronology is undetermined. U3 is characterized by various strong amplitudes and low frequency reflectors displaying a strong contrast with top depositional units. These reflectors show locally a divergent geometry similar to seaward dipping reflectors (SDRs). They are interpreted as volcanism or volcanoclastic sediments (Table 1).

In agreement with P-wave velocities model (Watremez et al., 2021), and the presence of volcano-sedimentary subsiding domains corresponding to the U1 and U2 seismic units, it is proposed that the western part of the profiles (eastern part of the SMCP) corresponds to thicker continental crust (Figure 2). Such an interpretation is also consistent with the presence of thin continental fine-grained red beds in the onshore wells (Salman & Abdula, 1995). Further east along the profiles, the location of U3 is the same as that of the thinned continental crust domain of Moulin et al. (2020). The continental crust is also characterized by deep highly reflective reflectors

Table 1
Summary of Key Observations of the Seismic Units, With Their Seismic Reflection Patterns and Ages

Stage	Label + Seismic pattern	Reflection characteristics					Interpretations	
		Boundaries	*Geometry*	*Continuity*	*Amplitude*	*Frequency*	*«Lithologies»*	*Ages*
T3	**Oceanic domain**							
	U5 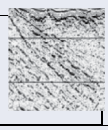	Top: offlaps Base: downlaps	Divergent	Continuous to discontinuous	Medium	Medium to high	Lava flows + sediments?	Mainly Lower Cretaceous
	U4 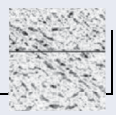	Top: Seldom defined Base: downlaps	CDRs & ODRs	Continuous to discontinuous	Medium to high	Low to medium	Gabbro - Magmatic faults	Lower Cretaceous
	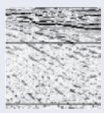	Top: Seldom defined Base: downlaps	Divergent OSDRs	Continuous	Low	Low to medium	Lava flows	Lower Cretaceous
	Continental Domain - *Divergence phase + Strike-slip component*							
T2+ T3?	U3 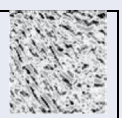	Top: offlaps Base: onlaps	Divergent SDRs ?	Continuous to discontinuous	Medium to high	Medium to high	Volcanic rocks - Volcanoclastic sediments	Jurassic to Lower Cretaceous?
T2	U2 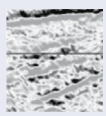	Top: erosional truncations Base: onlaps	Divergent	Continuous	Medium to high	High	Volcanic rocks	Lower Jurassic (ca. 180 Ma)
T1	U1 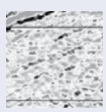	Top: toplaps & offlaps Base: onlaps	Divergent	Continuous	Medium to high	Low to medium	Sediments	Permian to Trias ?

Note. CDRs, Continentward Dipping Reflectors; ODRs, Oceanward Dipping Reflectors; OSDRs, Oceanic Seawards Dipping Reflectors; SDRs, Seawards Dipping Reflectors.

and, occasionally, slightly curved (see e.g., Figure 4). They may correspond to highly deformed basement or magmatic rocks.

4.2.2. The Oceanic Domain

Various seismic units are recognized along the eastern part of profiles (Figures 4–7) and along the N-S profile (Figure 8) below TAB and above strong and sub-continuous high amplitude reflectors located at a minimum of 3 s TWTT below TAB, reaching 4 s TWTT locally (Figure 6a). Interestingly, they become less marked and may disappear locally beneath the regions with rough basement topography, high-topography (see the proximal parts of the oceanic domain along Profiles #3 and #4, Figures 6 and 7) or well-developed seamounts (Figure 8). These reflectors are interpreted as the oceanic Moho (a classical time-depth migration would locate those reflectors at ca. 10 km depth).

The inner part of the oceanic crust (U4 - Table 1), well-recorded along the profile of Figure 8, is the superimposition of two geometrical patterns of the reflectors. The upper one, located below the TAB with a maximum thickness of 1 s TWTT, is characterized by oblique laterally accreting seismic reflectors bended toward the south. Their length is less than 10 km with a maximum height of 250 ms TWTT. Controlled by normal faults, these oblique reflectors flatten upward and may corresponds to oceanic seawards dipping reflectors (OSDRs, subset one in Figure 8b). The lower pattern of reflector geometries show reflectors dipping in opposite directions

alternating between dipping toward the continent (CDRs: continentward dipping reflectors; subset 2 in Figure 8b) and dipping toward the ocean (ODRs: oceanward dipping reflectors; subset 2 in Figure 8b). These oblique reflectors are generally five kilometers long, and merge with our interpreted oceanic Moho. A third layers exists between the OSDRs and the paired ODRs-CDRs: a seismic transparent interval (1.5 s TWTT thick) the bottom of which is a continuous strong reflector that in some places defines the upper limit of the ODRs-CDRs (orange line in Figure 8a). In addition, Figure 6 displays the same seismic characteristics, but the OSDRs are not controlled by normal faults (see subset 2). The OSDRs dip toward the east and are less than 10 km long. ODRs and CDRs, also locally present (subset 2, Figure 6a), are generally five kilometers long.

Along the southeastern edge of the SMCP (Figures 6 and 7), the outer part of the oceanic crust displays distinct seismic facies, U5 (Figures 6 and 7; Table 1). This unit consists of different groups of bright and coherent eastward dipping reflectors with medium amplitudes and medium frequency. Controlled by strike-slip faults, they show a remarkable divergent geometry pattern similar to the OSDRs, and are interpreted as lava flows (Table 1).

The presence of OSDRs, CDRs and ODRs together above a high amplitude deepest reflector interpreted as the oceanic Moho is typical of oceanic crust (Karson, 2002; Mutter & Carton, 2013; Sauter et al., 2021). This interpretation fits well with the presence of magnetic anomalies (Mueller & Jokat, 2019) in some places (Figure 2). In detail, the OSDRs may correspond to the progressive asymmetric subsidence of lava flows (Table 1, Karson, 2002) that could be associated locally with faults (subset 2 in Figure 8). Below, the abundance of ODRs may correspond to tilted grabbro whereas CDRs may be interpreted as syn-magmatic faults (Table 1, Bécel et al., 2015; Momoh et al., 2017, 2020; Sauter et al., 2021) which root into the oceanic Moho. Interestingly, these reflectors (OSDRs, CDRs and ODRs) and U5 seismic facies are primarily found in the over-thickened oceanic crust (deeper Moho) attesting to robust magma supply at some places.

4.3. Structural Features of the Margin From Seismic Profiles

4.3.1. The Continental Domain

The continental domain is at least 30-km thick (see Watremez et al., 2021) and is bounded to the east by a single major fault, Fault 1 (F1, Figure 2). This fault trends N-S and dips slightly toward the ocean. It is associated with a main escarpment which has a minimum extent of 300 km (i.e., approximately the distance between Profile #1 and Profile #4) with 1.5 s TWTT of relief locally (Figure 6a). To the south, this structure shows a negative flower-structure geometry (e.g., Figure 6a) suggesting a strike-slip component while it was active.

The continental domain of the Limpopo margin is affected by various sets of faults ranging from low-to high-angle dipping normal faults, but displaying the same N-S trend. U1 seems to be controlled by low-to moderate-angle faults whereas U2 is often bounded by high-angle faults (Figures 6 and 7). But, in the Profile #2 (Figure 5) U1 is also controlled by a high-angle fault that seems to be active during the formation of the two wedges (U1 and U2). This implies a strong structural inheritance of U1 faults from U2 faults. In any case, these faults, which dip toward the continent, control the formation of the U1 and U2 wedges.

The transitional continental domain is located to the east in between the F1 and Fault 2 (F2) (Figure 2), topped by a flat TAB surface (Figures 4–7). This zone of crustal thinning is wider to the south where it reaches a width of approximately 40 km (see Profile 1#, Figure 4 vs. Profile #4, Figure 7). It is characterized by a set of N-S trending faults which are more distinct in the northern part of the margin than in the south where they dip toward the continent. They are mainly associated with the SDRs formation (i.e., the U3 seismic unit, Table 1). They were probably active during and after formation of the major fault, F1.

4.3.2. The Oceanic Domain

The oceanic domain shows various sets of faults (normal, reverse and strike-slip; e.g., Figure 6) highlighting the variability of the tectonic regime over time. The first fault, F2, striking N-S and dipping toward the continent (Figure 4 through 7), corresponds to the lithospheric boundary between the thinned continental and oceanic domains. In some places, this major fault clearly controls the SDRs in the thinned continental crust as indicated by the wedge-shaped geometry (Figure 5). To the east on the oceanic crust, several strike-slip faults are observed leading up to the major Fault 3 (F3) that separates the thick oceanic crust without an oceanic Moho from oceanic crust with a clear Moho (e.g., Figures 5 and 6). All these faults control the formation of the OSDRs (see U4 seismic unit, Table 1) and are therefore interpreted as an oceanic transform fault system. Interestingly, the 3D

geometry of TAB forms an elongated high in-between F2 and F3, parallel to the strike of the transform faults zone. It corresponds to a small oceanic ridge where magmatic infilling occurs during transform motion that changes direction at chron M25. To the south, the uppermost Valanginian horizon onlaps the ridge suggesting a local uplift during transform activity.

5. Discussion

5.1. Margin Architecture Along the SMCP

Our set of seismic lines illustrates the principal crustal domains and the limits of the Limpopo continental margin which are also evident in the joint wide-angle seismic profiles (see Watremez et al., 2021). The SMCP continental crust thins sharply toward the east, defining a narrow necking zone. This necking zone changes from north to south, becoming broader to the south (toward the MR) with a width of 40 km (see Profile #1, Figure 4 vs. Profile #3, Figure 6). Unfortunately, Cretaceous magmatism along the MR masks structures. However, the tectonic setting and our interpretations indicate that the margin as a transform margin where F2 marks the boundary between the continental crust and oceanic crust.

5.1.1. Morphological Characteristics of the Limpopo Transform Margin

Most of recent studies of transform fault systems used bathymetric profiles to describe the structure of transform margins (e.g., Loncke et al., 2019; Mercier de Lepinay et al., 2016), but the current bathymetry represents on the final only the post-transform history. The distribution of the magnetic anomalies (Mueller & Jokat, 2019) indicates that the Limpopo transform margin was still active during the lowermost Cretaceous. At that time, this margin was characterized by the regional erosional surface (TE horizon) that displays a transition from flat to gentle slopes within the continental slope bound on the east by F1 (Figures 4–7). Such a feature may correspond to a so-called marginal plateau (Mercier de Lepinay et al., 2016), recently renamed as transform marginal plateau (Loncke et al., 2019). The Limpopo transform margin shows an initial stretching and thinning phase (e.g., during the Permo-Trias) prior to the initiation of transform motion and continental separation as has been suggested for other transform margins by Mercier de Lepinay et al. (2016). This transform marginal plateau cannot be explained by (a) an isostatic compensation of a thinned continental crust (Mercier de Lepinay et al., 2016), (b) differential thermal subsidence between the continental crust and the adjacent oceanic plate (Lorenzo & Wessel, 1997) or (c) by thermal uplift associated with the spreading center activity (e.g., Mascle & Blarez, 1987; Scrutton, 1979). Indeed, this regional vertical displacement is not correlated with the spreading center passage, because it probably started earlier during the intra-continental stage. Here, we propose that such regional uplift could be the ultimate record of topographic swells associated with mantle plume dynamic (e.g., Şengör, 2001). This hypothesis is consistent with some studies (e.g., De Wit, 2007; Nyblade & Robinson, 1994;), that attribute other younger major unconformities to dynamic mantle processes, such as the Late Cenomanian unconformity, a major denudation event that extended over large areas of thousands of kilometers.

Although marginal ridges often occur at transform margins (e.g., Basile et al., 1993; Basile & Allemand, 2002; Mercier de Lepinay et al., 2016), no clear marginal ridge was observed here. Conversely, increased subsidence during Valanginian time is recognized above the top of the thinned continental crust (e.g., Figure 7). This suggests a downward movement between F1 and F2, whereas a more elevated topography triggered by the transform zone activity is recorded in the most western part of the oceanic domain as far as F3 (e.g., Figure 7). Such morphology seems to minimize the thermal effect between the oceanic lithosphere and the continental one across the transform fault zone. Here, we suggest that crustal thickness variations between F1 and F3 may be primarily explained by a substantial ductile extraction of the lower crust as a result of the global high temperature thermal regime induced by the plume activity during transform fault zone activity (i.e., intra-continental transform fault stage and active transform margin stage). A similar process was invoked along the major transform margin southwest of the Grand Banks, off eastern Canada and in Salton Sea in southern California where pull-apart systems have been described (e.g., Brothers et al., 2009). In the first case, the continental crust was thinned by a factor of three within the sharp transition between continental and oceanic regions (Keen et al., 1990). This hypothesis is also supported by 3D finite element thermal-kinematic modeling results from Henk and Nemčok (2016). Their results show that ductile extraction of the lower crust at transform margin can lead to lateral variations of uplift/subsidence, in upper- and lower-crustal layers and also the depth of the Moho. In the second case, using seismic

reflection data and geological observations, Brothers et al. (2009) reported differential subsidence (an asymmetric basin) in Salton Sea in southern California associated with oblique extension across strike-slip faults.

5.1.2. Structural Style of the Limpopo Transform Margin: The Transform Fault Zone

This study shows that the transform fault zone affects both thinned continental and oceanic domains, preserving both the intra-continental transform fault stage and the active transform margin stage. The right-lateral motion component of the Limpopo Transform Fault Zone (LTFZ) associated with the oblique direction of extension led to a widening of the LFTZ to include several faults organized in a flower structure forming a zone of deformation. Such deformation also induces an asymmetry between a narrow inner corner (i.e., transform divergent intersection; e.g., Figure 2) and a wide outer corner, where large area of thinned continental crust may be mapped (see relatively flat TAB surface between F1 and F2 in the seismic lines). This is consistent with the cumulated strike-slip deformation, which clearly increases toward the south as evidenced by the numerous strike-slip faults (see Profile 1#, Figure 4 vs. Profile #4, Figure 7). This movement is also consistent with the migration of Antarctica with respect to Africa (i.e., NW-SE and N-S direction; Davis et al., 2016; Klimke et al., 2018; Mueller & Jokat, 2019; Nguyen et al., 2016).

To the north, the transform fault zone abuts the NE-SW trending Beira High segment. According to our seismic interpretations, the inner corner of this intersection is made of horsetail transfer structures (Figure 10) that connect strike-slip and normal faults at the tip of the intra-continental rift zone. These NW-SE trending faults that define a transfer fault zone (Figure 2), accommodate relative displacement between NE-SW trending rifted segments. Interestingly, the major transfer structures trend approximately N-S along the Limpopo margin. They are therefore oblique to the previous ones (Figure 2). Thus, these faults which also define a major transfer fault zone are not parallel to the relative plate displacement suggesting that their geometry may be affected by pre-existing anisotropy (e.g., Nemčok et al., 2016). Therefore, the obliquity between the relative plate motion (N-S) and the regional trend (NW-SE) at divergent plate boundary does not prevent the formation of a transform system. South of the SMCP, the segment merges with the submarine volcanics of the Mozambique Plateau area (i.e., the MR, the Mozambique F.Z., Figure 1) and focus magmatic activity.

Three principal fault strands defining the Limpopo transform fault zone from west to east are interpreted as follows.

1. The western fault strand: F1 is intra-continental (i.e., belongs to the intra-continental transform fault stage) and separates the thick continental crust from the thinned crust. It is located along the SMCP and may be extended southwards at least as far as the Arial graben (Figure 1) where it is probably connected to the Natal divergent segment. This sub-vertical N-S trending fault exposes a flower structure indicating strike-slip deformation.
2. The primary fault strand: F2 is the main plate boundary between, the Mozambique Basin and the adjacent Limpopo and north Natal continental margins. This continental-oceanic transform fault dips toward the west and trends N-S, and thus corresponds to the active transform margin stage that starts coincident with the onset of seafloor spreading.
3. The eastern fault strand: F3 is located in the oceanic domain, separating a more typical oceanic crust (8–9 km thick, Figure 7b) with a clear oceanic Moho from a thicker oceanic crust (13 km thick, Figure 7b) without a clear Moho reflector on seismic reflection profiles. This segment thus corresponds to the more oceanic part of the transform fault zone that develops with respect to the global transtensional deformation.

Between F1 and F2, several magmatic events and strike-slip faults activities are evident. The obliquity to the margin of relative plate motion and the regional trend of the rift is accommodated by oblique structures forming pull-apart basins that favor the emplacement of magmatic infilling during the continental rifting. This implies that a significant and localized magma supply in the thinned continental domain may have focuses extensional deformation as has been suggested by previous studies in other locations (e.g., Buck, 1991; Ebinger & Casey, 2001; Leroy et al., 2010). Between F2 and F3, various strike-slip faults with normal components of motion affected the oceanic crust during spreading. Thus, this suggests that the zone of deformation continued to develop eastward, close to the F2, widening toward the south to the LTFZ.

5.2. Crustal Domains Along the Limpopo Transform Margin

5.2.1. Nature and Age of Crustal Domains

The continental domain is characterized by tilted blocks with associated syn-rift rocks and a thickness of the crust of 30 km (Watremez et al., 2021). The continental basement along the SMCP may reasonably be thought of as an extension of the Archean crust of the Meso-Neoproterozoic Namaqua-Natal (South Africa) and Mozambican crust (Figure 1; Hanson, 2003). Interestingly, Watkeys and Sokoutis (1998) observed that faults of possible Early Jurassic (180–175 Ma) age on the Archean Craton are organized along N-S trends whereas transtension occurred in the Naquala-Natal orogenic belt with ENE strike-slip movement along the southeastern margin of Africa (Figure 1). Our map (Figure 2) shows the presence of Early Jurassic N-S fault trending along (i) the SMCP and (ii) the modern outcropping basement of the Early Jurassic volcanic rocks (i.e., the Lebombo Monocline, Figure 1), suggesting that these faults are probably the north-eastward extension of the fault pattern described by Watkeys and Sokoutis (1998) in the Archean Craton. Consequently, the continental crust may partly correspond to the eastward extension of the Archean Kaapval Craton below the SMCP. Considering the presence of a cratonic continental crust below this area, the Antarctica must be placed further to the south than has been proposed by previous models (e.g., Eagles & König, 2008; Gaina et al., 2013; Jacobs & Thomas, 2004; König & Jokat, 2006; Leinweber & Jokat, 2012; Nguyen et al., 2016; Reeves et al., 2016; Reeves, 2017; Seton et al., 2012).

Further, according to our new argon ages (180.3 ± 0.8 Ma and 178.9 ± 1.4 Ma), U2 can be reasonably interpreted as part of the LIP. Thus, the U1 unit may be connected with a previous rifting event such as the Permo-Triassic Karoo extension. Conversely, interpreted as SDRs, the age of U3 unit remains poorly constrained. Such formations occurred probably between 180 Ma and the first identified magnetic anomaly along the SMCP, M25 or 156 Ma (Mueller & Jokat, 2019). We cannot exclude the possibility that recent magmatic activity related to F2 may overprint these previous magmatic events (e.g., the LIP).

The oceanic domain is found east of F2, where oceanic magnetic anomalies M25 to M0 are well-expressed in the Mozambique Basin (Figure 1). It is characterized by post-rift sediments ranging from 1 to 2 s TWTT of thickness along the SMCP (Figure 8). The oceanic crust shows a southward thickening at around M17r or 143 Ma (Mueller & Jokat, 2019) with a Moho depth ranging from 2.25 to 3.5 s TWTT below TAB, approximately 4.5 km difference in thickness (Figure 8). Such differences of architecture may be related to a change of the dynamic of oceanic spreading during the Lower Cretaceous ∼143 Ma.

5.2.2. Magmatism Along the Limpopo Transform Margin

The large volume of magmatic activity in the SMCP and Natal Valley implies hot thermal regime since the onset of rifting at ca. 180 Ma (e.g., the volcanic series of the Lebombo, Figure 1) probably related to mantle plume activity (Storey & Kyle, 1997; White & McKenzie, 1989; White, 1997). Distributed strike-slip deformations coeval with the magma emplacement (U2, SDRs, elongated oceanic ridge parallel to the relative motion) argues for a hot and weak crust supported by flowing asthenosphere within the transform zone. The tectonic activity may also enhance such particular thermal conditions locally. Indeed, the spatial alignment of volcanism and lithospheric- and/or crustal-faults location suggests that the location and the amount of magmatic activity are probably influenced by the tectonic setting. We propose that different types of faults (e.g., transfer and transform faults) may have induced and localized crustal thinning (e.g., the thinned crust between the F1 and F2) and as a consequence, lithospheric thinning, which increased the amount of magmatic activity locally. Based upon the sum on this evidence for magmatic activity during the entire evolution of the transform margin, we propose that the Limpopo transform margin be considered as a magma-rich margin which had a continuous of magma, similar to magma-rich rifted margin (Skogseid et al., 1992; White & McKenzie, 1989). Thus, we defined here a new type of margin: the magma-rich transform margin.

5.3. Regional Implications

Based on our observations and previously published data (see our simplified geodynamic chart in Figure 9), we propose a new scenario of formation and evolution for the Limpopo transform margin with geodynamic implications for the offshore regions of the Beira High and Angoche margin segments (Figure 11). This scenario is constrained by (a) the oblique migration of Antarctica with respect to Africa in two stages: NW-SE extension that rotates to N-S at around chron M25 or 156 M as evidenced by the trend of magnetic anomalies and the trend of

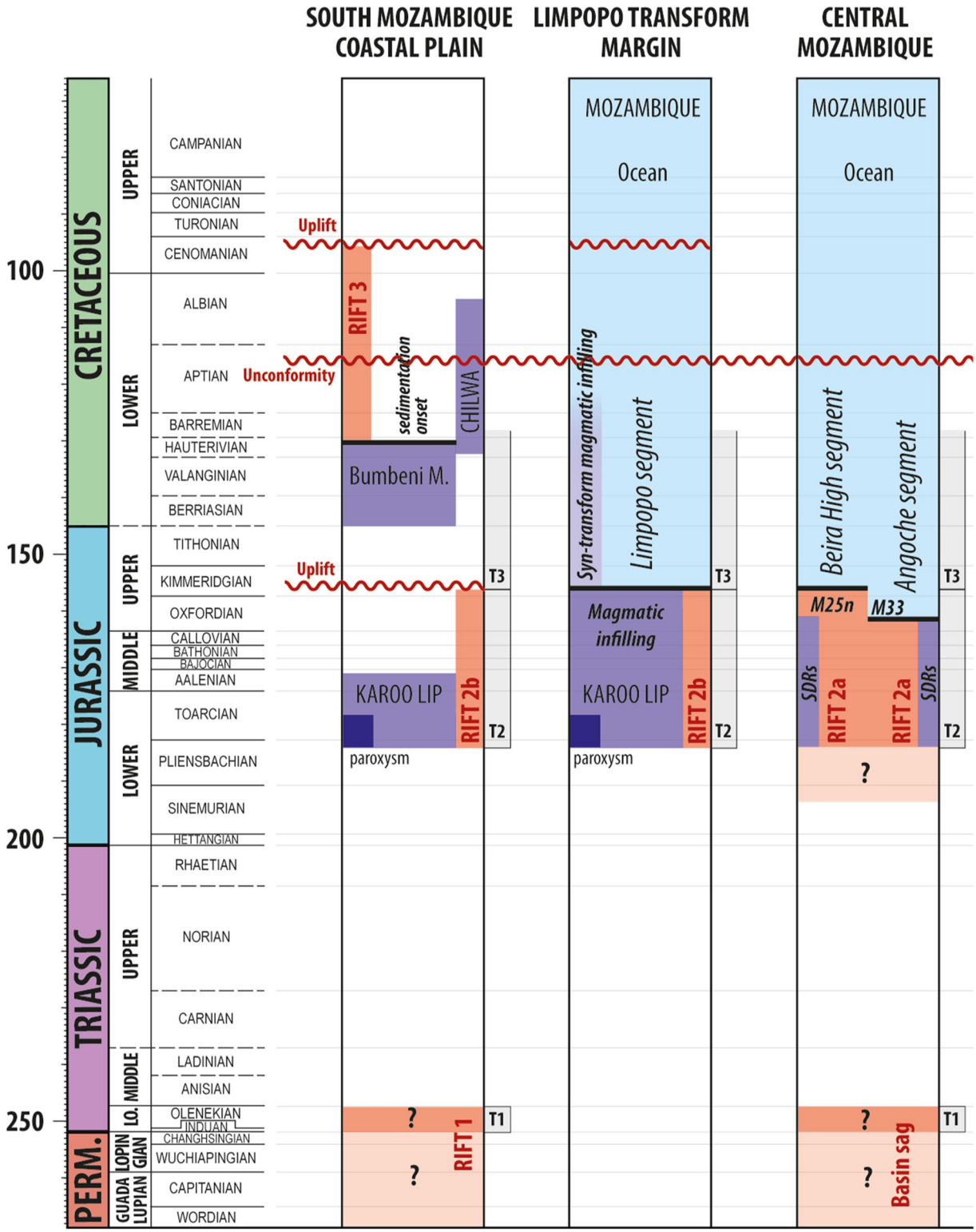

Figure 9. Simplified geodynamic chart. The violet color represents different magmatic systems (the ages of the LIP are from Jourdan et al. (2007); the ages of the Bumbeni/Movene province are from Saggerson and Bristow (1983) and Allsopp et al. (1984); the ages of the Chilwa province are from Flores (1964) and Eby et al. (1995). Red color represents a rifting period. Rift2a is an orthogonal rifting. Rift2b is an hyper-oblique rifting. Blue color represents the ocean marked by the onset of oceanic spreading at chron M25n and M33n (Senkans et al., 2019). Magnetic isochrons are from Mueller and Jokat (2019). Uplifts and unconformity are described in Ponte et al. (2019).

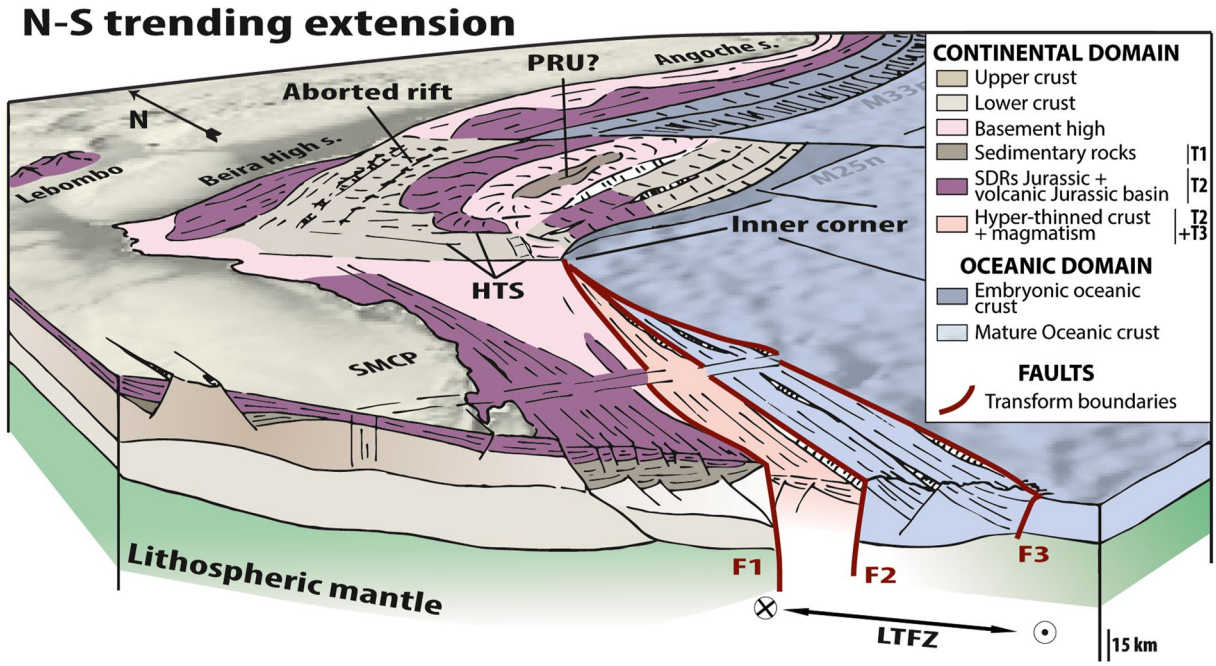

Figure 10. Synthetic 3D bloc diagram showing the basement structures, syn-rift deposits and magmatism during the transform stage that corresponds to the Limpopo transform margin activity. This sketch is consistent with our structural map in Figure 2 showing the segmentation of the Mozambique margins with, from west to east the Limpopo, the Beira High and Angoche margin segments. Horsetail Transfer Structures (HTS), Limpopo East (LE), Limpopo Main (LM), Limpopo Transform Fault Zone (LTFZ), Limpopo West (LW), Pre-Rift Unit (PRU), South Mozambique Coastal Plain (SMCP), Segment (s).

transform segments and by (b) intense magmatic activity during the Early Jurassic related to the emplacement of a mantle plume and marked by flooding of the LIP lava at ca. 183 Ma (e.g., our data; Jourdan et al., 2007; Riley et al., 2004; Storey & Kyle, 1997; Svensen et al., 2012; White & McKenzie, 1989; White, 1997).

5.3.1. The Pre-Breakup History: Permo-Triassic Failed Rift (T_1 Stage)

Offshore data along the SMCP (see profiles #1 – #4, Figure 4 through 7) show that the sediments (U1 unit) are controlled by N-S trending listric to low-angle normal faults (e.g., Figures 2 and 7). Considering that the overlying prism corresponds to the LIP, the age of the deepest wedge is earlier and probably related to the Permo-Triassic event, which is well-known in the whole east Africa (Figure 1) (e.g., Castaing, 1991; Cox, 1992; Daly et al., 1989, 1991; Macgregor, 2018; Watkeys, 2002). For example, offshore data along the Beira High segment also indicate the presence of older deposits, which are not related to the NE-SW trending faults linked to NW-SE trending extension activity developing during the Early Jurassic (Mahanjane, 2012; Senkans et al., 2019). Based on seismic reflection interpretations, these studies show that deformation related to such older deposits occurred before the Middle Jurassic syn-rift stage, and therefore may correspond to Permo-triassic sediment deposits in age (Figure 10).

This T_1 stage (Figures 11a) may be related to intra-continental tectonics compatible with E-W (e.g., Daly et al., 1989, 1991) and/or NW-SE trending extension (Castaing, 1991). The record of this deformation in the SMCP is N-S trending faults similar to the ones of the southern part of the Lebombo. Probably due to Proterozoic inheritance, this deformation is differently recorded north of Mozambique (Figure 1), with faults pattern varying from NE-SW trending along the Limpopo belt to E-W in the Cabora Bassa Basin and from NW-SE trending between the Angoche and Beira-High margin segments (Figure 1).

5.3.2. Break-Up History to the Formation of the First Oceanic Crust (T_2 Stage, 183–156 Ma)

The role of pre-existing structures along the SMCP is difficult to document but our seismic data shows occasionally that same faults controlled U1 and U2 deposits, implying that pre-existing structures played a role in the future rift segmentation (Figures 11b). Similar features are reported along the Angoche and Beira-High offshore margin segments. They are separated by NW-SE trending transfer fault (Figure 2), which are in lined with the onshore Permo-Triassic NW-SE trending faults mapped south of Malawi (Figure 1). This implies that the

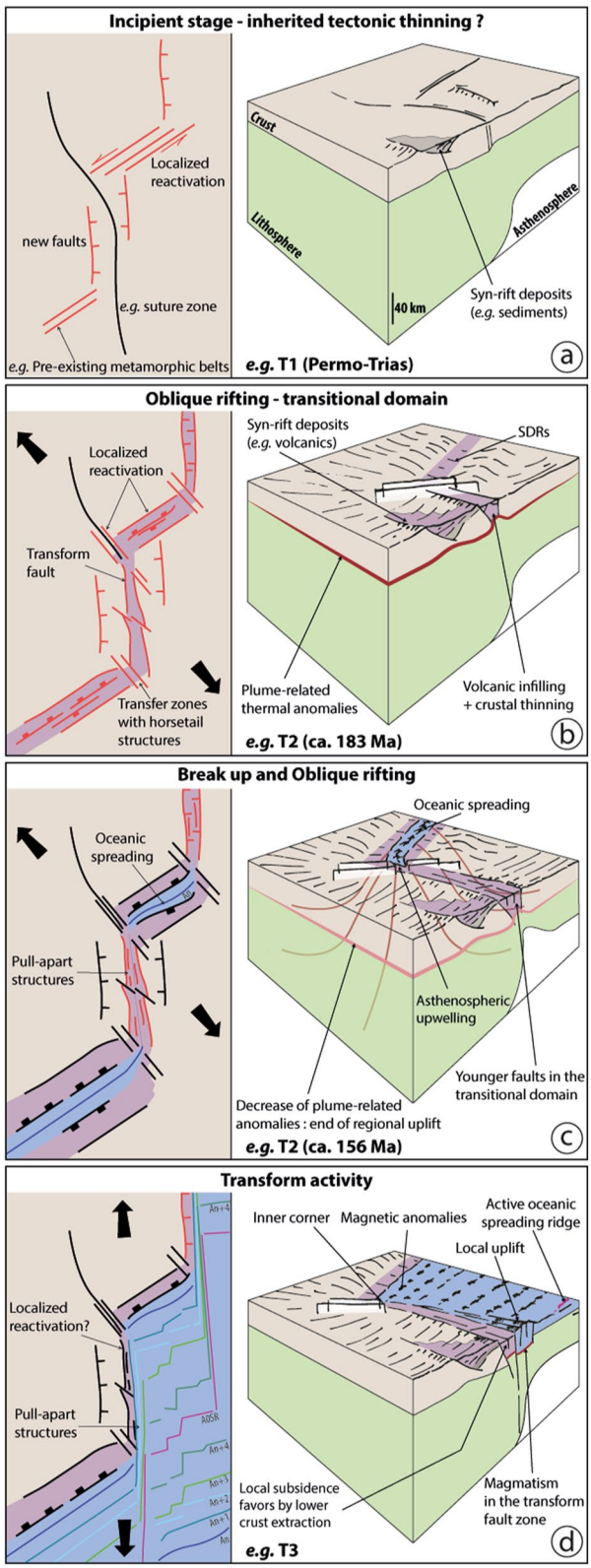

Figure 11. Conceptual model of the Limpopo magma-rich transform margin evolution from the (a) incipient stage to (d) final stage in map view and in 3D. Note that uplifts are mainly supported by mantle flows that could be triggered by a plume. An (Identified Oceanic Magnetic anomaly).

Permo-Triassic rifts played a role in the mechanisms of rift propagation and subsequent continental breakup at southern African-scale.

Stage T_2 starts with the LIP onset, with lava flows at ca. 183 Ma (e.g., Jourdan et al., 2007; Svensen et al., 2012; Riley et al., 2004). It is mainly characterized by half-grabens (made up of U2 seismic unit, Table 1) bounded by early Jurassic N-S trending faults and coeval with the onset of F1 (Figure 10). Our seismic data show also that continental crust and Permo-Triassic sediments are locally intruded by magma that could be associated with the mantle plume (Figures 5 and 7).

Magmatic SDRs were also described in the same chronological setting as these half-grabens and are therefore of Early to lowermost Upper Jurassic age (Figures 10 and 11b), that is before chron M25 (156 Ma). But these volcanics were emplaced in a different tectonic context from those found in the N-S trending half-grabens located on the continental crust. Indeed, most of them (along the southwest Beira High and Angoche magma-rich segments, Figure 10; see Senkans et al., 2019) are related to NE-SW trending normal faulting of the extended continental crust. They can also be recognized along the eastern part of LTFZ (U3 unit, Table 1) which records transtensional deformation corresponding to the accommodation zone between the two divergent segments of Angoche-Beira High and Natal during the intra-continental transform fault stage (Figures 11b and 11c). While, both Beira High and Natal Valley segments display the same geometry, the timing of the seafloor spreading along the Natal Valley remains unclear.

5.3.3. Spreading and Transform Plate Boundary History (T_3 Stage <155 Ma)

Stage T_3 (Figures 11d) corresponds to the steady-state oceanic seafloor spreading with a plate movement rotating from NW-SE to N-S as testified magnetic anomalies (e.g., Cox, 1992; Klimke et al., 2018; Nguyen et al., 2016; Reeves, 2017), indicating that Antarctica was moving SSE with respect to Africa. Stage T_3 marks, therefore, the onset of the transform activity along the SMCP at chron M25 whereas oceanic spreading is ongoing in the Angoche, Beira High and probably in the Natal margin segments (Figure 9). Here, the continent-ocean transition is more or less parallel to the intra-continental transform fault (Figures 11c). Hence, the pre-existing transfer fault seems to guide the trend, the structural style and maybe also the location of the principal future transform fault.

While the Angoche and Beira High margins recorded a period of quiescence (post-rift phase), the continental part of the Limpopo margin was going through an episode of uplift related to plume activity (see TE surface in Figures 4–7) and its distal oceanic part records magmatic infilling related to strike-slip faults (U5 facies, Table 1) in-between F2 and F3 (Figure 10). In other words, the cumulate strike-slip deformation related to a dextral transtensional movement increases toward the south through time forming a 13 km-thick magmatic oceanic crust with an elongated ridge, which is characterized by a set of oceanic transform faults controlling fan-shape magmatic infilling (Figures 11d). Interestingly, the peculiar thermal conditions induced by the plume activity does not seem to have prevented the later formation of the continent-ocean transform fault zone.

6. Conclusion

We used a high-resolution multichannel seismic data set provided by industry with calibration wells to better understand the structure and evolution of the continental scale dextral strike-slip system of the Limpopo transform margin in South Mozambique from rifting, to oceanic spreading, to transform. We propose (i) a new classification of oblique margin and (ii) a three stages tectonic evolution of the margin from the Permo-Triassic to Early Cretaceous times.

1. We propose the term "magma-rich" for the Limpopo transform margin case.
   The magma-rich Limpopo transform margin shows that necking is primarily controlled by a system of strike-slip structures (syn-transfer and -transform faults) rather than a single transform. Such extensional pattern allows magmatic feeding and infilling during the whole transform evolution stage. This excess magmatic activity contributed significantly to focus extension in the crust and vice versa.
   The magma-rich Limpopo transform margin displays a clear magmatic signature. Large-scale differential subsidence along the margin may be explained by mantle dynamics whereas substantial lower crustal extraction may be invoked at a smaller-scale.
2. The Limpopo transform margin recorded different deformation stages from the Permo-Triassic to Cretaceous times.
   The first stage (T_1) corresponds to the onset of the continental stretching at time of the Karoo Rifts formation (mainly Early Triassic) and is characterized by half-grabens that are compatible with an E-W and/or NW-SE trending extension.
   At time of the LIP (ca. 180 Ma) a NNW-SSE extension regime prevailed up to the lowermost Late Jurassic (T_2), and the rifting was oblique to the orientation of the Limpopo margin. This stage is characterized by the deposition of volcanic wedges ranging from around 180 Ma (180.3 $\pm$ 0.8 Ma and 178.9 $\pm$ 1.4 Ma according to our new argon ages) to 156 Ma.
   The last stage (T_3), Late Jurassic to Early Cretaceous in age, corresponds to the opening of the Mozambique Basin on its western side at 156 Ma, the time of Limpopo transform fault zone onset. The SSE displacement of Antarctica with respect to Africa is accommodated by a transtensional deformation along the SMCP which significantly contributes to the distribution of magma.

Data Availability Statement

Data interpretations used in this paper are available from data repository Seanoe.org (https://doi.org/10.17882/76414).

Acknowledgments
Vincent Roche was supported by a grant from the PAMELA project and by Sorbonne University. The PAMELA project (PAssive Margin Exploration Laboratories) is a scientific project led by Ifremer and TOTALENERGIES in collaboration with Université de Bretagne Occidentale, Université Rennes 1, Sorbonne Université, CNRS and IFPEN. We also thank Charlie Kergaravat, Jean-Claude Ringenbach and François Sapin at Totalenergies for insightful discussions and seismic interpretation assistance. We thank Dieter Franke, Ameha Atnafu Muluneh, David Iacopini and an anonymous reviewer for their assistance in evaluating and improving this manuscript. We deeply thank Dr Heather Sloan for post-editing the English style and grammar.

References

Abdelmalak, M. M., Planke, S., Faleide, J. I., Jerram, D. A., Zastrozhnov, D., Eide, S., & Myklebust, R. (2016). The development of volcanic sequences at rifted margins: New insights from the structure and morphology of the Vøring Escarpment, mid-Norwegian Margin. *Journal of Geophysical Research: Solid Earth*, *121*(7), 5212–5236. https://doi.org/10.1002/2015JB012788

Allsopp, H. L., Manton, W. I., Bristow, J. W., & Erlank, A. J. (1984). *Rb-Sr Geochronology of Karoo Felsic Volcanics. Petrog. Volcan* (Vol. 13). Rocks Karoo Prov. Spec. Publ. Geol. Soc.South Africa.

Baby, G., Guillocheau, F., Morin, J., Ressouche, J., Robin, C., Broucke, O., & Dall'Asta, M. (2018). Post-rift stratigraphic evolution of the Atlantic margin of Namibia and South Africa: Implications for the vertical movements of the margin and the uplift history of the South African Plateau. *Marine and Petroleum Geology*, *97*, 169–191. https://doi.org/10.1016/j.marpetgeo.2018.06.030

Basile, C. (2015). Transform continental margins—Part 1: Concepts and models. *Tectonophysics*, *661*, 1–10. https://doi.org/10.1016/j.tecto.2015.08.034

Basile, C., & Allemand, P. (2002). Erosion and flexural uplift along transform faults. *Geophysical Journal International*, *151*(2), 646–653. https://doi.org/10.1046/j.1365-246X.2002.01805.x

Basile, C., Mascle, J., Popoff, M., Bouillin, J. P., & Mascle, G. (1993). The Ivory Coast-Ghana transform margin: A marginal ridge structure deduced from seismic data. *Tectonophysics*, *222*(1), 1–19. https://doi.org/10.1016/0040-1951(93)90186-N

Bécel, A., Shillington, D. J., Nedimović, M. R., Webb, S. C., & Kuehn, H. (2015). Origin of dipping structures in fast-spreading oceanic lower crust offshore Alaska imaged by multichannel seismic data. *Earth and Planetary Science Letters*, *424*, 26–37. https://doi.org/10.1016/j.epsl.2015.05.016

Ben-Avraham, Z. C. J. H., Hartnady, C. J. H., & Le Roex, A. P. (1995). Neotectonic activity on continental fragments in the southwest Indian Ocean: Agulhas Plateau and Mozambique Ridge. *Journal of Geophysical Research: Solid Earth*, *100*(B4), 6199–6211. https://doi.org/10.1029/94JB02881

Bird, D. (2001). Shear margins Continent-ocean transform and fracture zone boundaries. *The Leading Edge*, *20*(2), 150–159. https://doi.org/10.1190/1.1438894

Brothers, D. S., Driscoll, N. W., Kent, G. M., Harding, A. J., Babcock, J. M., & Baskin, R. L. (2009). Tectonic evolution of the Salton Sea inferred from seismic reflection data. *Nature Geoscience*, *2*(8), 581–584. https://doi.org/10.1038/ngeo590

Buck, W. R. (1991). Modes of continental lithospheric extension. *Journal of Geophysical Research*, *96*(B12), 20161–20178. https://doi.org/10.1029/91JB01485

Castaing, C. (1991). Post-Pan-African tectonic evolution of South Malawi in relation to the Karroo and recent East African rift systems. *Tectonophysics*, *191*(1–2), 55–73. https://doi.org/10.1016/0040-1951(91)90232-H

Catuneanu, O., Wopfner, H., Eriksson, P. G., Cairncross, B., Rubidge, B. S., Smith, R. M. H., & Hancox, P. J. (2005). The Karoo basins of south-central Africa. *Journal of African Earth Sciences*, *43*(1–3), 211–253. https://doi.org/10.1016/j.jafrearsci.2005.07.007

Cawood, P. A., & Buchan, C. (2007). Linking accretionary orogenesis with supercontinent assembly. *Earth-Science Reviews*, *82*(3–4), 217–256. https://doi.org/10.1016/j.earscirev.2007.03.003

Clerc, C., Ringenbach, J. C., Jolivet, L., & Ballard, J. F. (2018). Rifted margins: Ductile deformation, boudinage, continentward-dipping normal faults and the role of the weak lower crust. *Gondwana Research*, *53*, 20–40. https://doi.org/10.1016/j.gr.2017.04.030

Cleverly, R. W., & Bristow, J. (1979). Revised volcanic stratigraphy of the Lebombo monocline. *South African Journal of Geology*, *82*(2), 227–230.

Collins, A. S., & Pisarevsky, S. A. (2005). Amalgamating eastern Gondwana: The evolution of the Circum-Indian Orogens. *Earth-Science Reviews*, *71*(3–4), 229–270. https://doi.org/10.1016/j.earscirev.2005.02.004

Cox, K. G. (1992). Karoo igneous activity, and the early stages of the break-up of Gondwanaland. *Geological Society, London, Special Publications*, *68*, 137–148. https://doi.org/10.1144/GSL.SP.1992.068.01.09

Daly, M. C., Chorowicz, J., & Fairhead, J. D. (1989). Rift basin evolution in Africa: The influence of reactivated steep basement shear zones. *Geological Society London, Special Publications*, *44*, 309–334. https://doi.org/10.1144/GSL.SP.1989.044.01.17

Daly, M. C., Lawrence, S. R., Kimun'a, D., & Binga, M. (1991). Late Palaeozoic deformation in central Africa: A result of distant collision? *Nature*, *350*(6319), 605–607. https://doi.org/10.1038/350605a0

Daszinnies, M. C., Jacobs, J., Wartho, J. A., & Grantham, G. H. (2009). Post Pan-African thermo-tectonic evolution of the north Mozambican basement and its implication for the Gondwana rifting. Inferences from 40Ar/39Ar hornblende, biotite and titanite fission-track dating. *Geological Society, London, Special Publications*, *324*(1), 261–286. https://doi.org/10.1144/sp324.18

Davis, J. K., Lawver, L. A., Norton, I. O., & Gahagan, L. M. (2016). New Somali Basin magnetic anomalies and a plate model for the early Indian Ocean. *Gondwana Research*, *34*, 16–28. https://doi.org/10.1016/j.gr.2016.02.010

Davison, I., & Steel, I. (2018). Geology and hydrocarbon potential of the East African continental margin: A review. *Petroleum Geoscience*, *24*(1), 57–91. https://doi.org/10.1144/petgeo2017-028

De Putter, T., & Ruffet, G. (2020). Supergene manganese ore records 75 Myr-long Campanian to Pleistocene geodynamic evolution and weathering history of the Central African Great Lakes Region–Tectonics drives, climate assists. *Gondwana Research*, *83*, 96–117. https://doi.org/10.1016/j.gr.2020.01.021

De Putter, T., Ruffet, G., Yans, J., & Mees, F. (2015). The age of supergene manganese deposits in Katanga and its implications for the Neogene evolution of the African Great Lakes Region. *Ore Geology Reviews*, *71*, 350–362. https://doi.org/10.1016/j.oregeorev.2015.06.015

De Wit, M. (2007). The Kalahari Epeirogeny and climate change: Differentiating cause and effect from core to space. *South African Journal of Geology*, *110*(2–3), 367–392. https://doi.org/10.2113/gssajg.110.2-3.367

Duncan, R. A., Hooper, P. R., Rehacek, J., Marsh, J. S., & Duncan, A. R. (1997). The timing and duration of the Karoo igneous event, southern Gondwana. *Journal of Geophysical Research - Solid Earth*, *102*(B8), 18127–18138. https://doi.org/10.1029/97JB00972

Eagles, G., & König, M. (2008). A model of plate kinematics in Gondwana breakup. *Geophysical Journal International*, *173*(2), 703–717. https://doi.org/10.1111/j.1365-246X.2008.03753.x

Ebinger, C. J., & Casey, M. (2001). Continental breakup in magmatic provinces: An Ethiopian example. *Geology*, *29*(6), 5272–5530. https://doi.org/10.1130/0091-7613(2001)029<0527:cbimpa>2.0.co;2

Eby, G. N., Roden-Tice, M., Krueger, H. L., Ewing, W., Faxon, E. H., & Woolley, A. R. (1995). Geochronology and cooling history of the northern part of the Chilwa Alkaline Province, Malawi. *Journal of African Earth Sciences*, *20*(3–4), 275–288. https://doi.org/10.1016/0899-5362(95)00054-W

Encarnación, J., Fleming, T. H., Elliot, D. H., & Eales, H. V. (1996). Synchronous emplacement of Ferrar and Karoo dolerites and the early breakup of Gondwana. *Geology*, *24*(6), 5352–5538. https://doi.org/10.1130/0091-7613(1996)024<0535:SEOFAK>2.3.CO;2

Fischer, M. D., Uenzelmann-Neben, G., Jacques, G., & Werner, R. (2016). The Mozambique Ridge: A document of massive multi-stage magmatism. *Geophysical Journal International*, *208*, 449–467. https://doi.org/10.1093/gji/ggw403

Flores, G. (1964). On the age of the Lupata rocks, lower Zambezi River, Mozambique. *Transactions of the Geological Society of South Africa*, *67*, 111–118.

Flores, G. (1984). The SE Africa triple junction and the drift of Madagascar. *Journal of Petroleum Geology*, *7*(4), 403–418. https://doi.org/10.1111/j.1747-5457.1984.tb00885.x

Francheteau, J., & Le Pichon, X. (1972). Marginal fracture zones as structural framework of continental margins in South Atlantic Ocean. *AAPG Bulletin*, *56*(6), 991–1007. https://doi.org/10.1306/819a40a8-16c5-11d7-8645000102c1865d

Gaina, C., Torsvik, T. H., van Hinsbergen, D. J., Medvedev, S., Werner, S. C., & Labails, C. (2013). The African Plate: A history of oceanic crust accretion and subduction since the Jurassic. *Tectonophysics*, *604*, 4–25. https://doi.org/10.1016/j.tecto.2013.05.037

Galasso, F., Pereira, Z., Fernandes, P., Spina, A., & Marques, J. (2019). First record of Permo-Triassic palynomorphs of the N'Condédzi sub-basin, Moatize-Minjova Coal Basin, Karoo Supergroup, Mozambique. *Revue de Micropaleontologie*, *64*, 100357. https://doi.org/10.1016/j.revmic.2019.05.001

Gohl, K., Uenzelmann-Neben, G., & Grobys, N. (2011). Growth and dispersal of a southeast African large igneous province. *South African Journal of Geology*, *114*(3–4), 379–386. https://doi.org/10.2113/gssajg.114.3-4.379

Hanes, J. A., York, D., & Hall, C. M. (1985). An 40Ar/39Ar geochronological and electron microprobe investigation of an Archean pyroxenite and its bearing on ancient atmospheric compositions. *Canadian Journal of Earth Sciences*, *22*(7), 947–958. https://doi.org/10.1139/e85-100

Hanson, R. E. (2003). Proterozoic geochronology and tectonic evolution of southern Africa. *Geological Society, London, Special Publications*, *206*(1), 427–463. https://doi.org/10.1144/GSL.SP.2003.206.01.20

Hanyu, T., Nogi, Y., & Fujii, M. (2017). Crustal formation and evolution processes in the Natal Valley and Mozambique Ridge, off South Africa. *Polar Science*, *13*, 66–81. https://doi.org/10.1016/j.polar.2017.06.002

Henk, A., & Nemčok, M. (2016). Lower-crust ductility patterns associated with transform margins. *Geological Society, London, Special Publications*, *431*(1), 361–375. https://doi.org/10.1144/sp431.9

Jacobs, J., & Thomas, R. J. (2004). Himalayan-type indenter-escape tectonics model for the southern part of the late Neoproterozoic–early Paleozoic East African–Antarctic orogen. *Geology*, *32*(8), 721–724. https://doi.org/10.1130/G20516.1

Jokat, W., Boebel, T., König, M., & Meyer, U. (2003). Timing and geometry of early Gondwana breakup. *Journal of Geophysical Research*, *108*(B9). https://doi.org/10.1029/2002JB001802

Jourdan, F., Féraud, G., Bertrand, H., Watkeys, M. K., & Renne, P. R. (2007). Distinct brief major events in the Karoo large igneous province clarified by new $^{40}Ar/^{39}Ar$ ages on the Lesotho basalts. *Lithos*, *98*, 195–209. https://doi.org/10.1016/j.lithos.2007.03.002

Karson, J. A. (2002). Geologic structure of the uppermost oceanic crust created at fast-to intermediate-rate spreading centers. *Annual Review of Earth and Planetary Sciences*, *30*(1), 347–384. https://doi.org/10.1146/annurev.earth.30.091201.141132

Keen, C. E., Kay, W. A., & Roest, W. R. (1990). Crustal anatomy of a transform continental margin. *Tectonophysics*, *173*(1–4), 527–544. https://doi.org/10.1016/0040-1951(90)90244-3

Klausen, M. B. (2009). The Lebombo monocline and associated feeder dyke swarm: Diagnostic of a successful and highly volcanic rifted margin? *Tectonophysics*, *468*, 42–62. https://doi.org/10.1016/j.tecto.2008.10.012

Klimke, J., Franke, D., Estevão, S. M., & Leitchenkov, G. (2018). Tie points for Gondwana reconstructions from a structural interpretation of the Mozambique Basin, East Africa and the Riiser-Larsen Sea, Antarctica. *Solid Earth*, *9*(1), 25–37. https://doi.org/10.5194/se-9-25-2018

König, M., & Jokat, W. (2006). The Mesozoic breakup of the Weddell Sea. *Journal of Geophysical Research*, *111*(B12). https://doi.org/10.1029/2005JB004035

König, M., & Jokat, W. (2010). Advanced insights into magmatism and volcanism of the Mozambique Ridge and Mozambique Basin in the view of new potential field data. *Geophysical Journal International*, *180*, 158–180. https://doi.org/10.1111/j.1365-246X.2009.04433.x

Leinweber, V. T., & Jokat, W. (2011). Is there continental crust underneath the northern Natal Valley and the Mozambique Coastal Plains? *Geophysical Research Letters*, *38*(14). https://doi.org/10.1029/2011GL047659

Leinweber, V. T., & Jokat, W. (2012). The Jurassic history of the Africa-Antarctica corridor - New constraints from magnetic data on the conjugate continental margins. *Tectonophysics*, *530–531*, 87–101. https://doi.org/10.1016/j.tecto.2011.11.008

Leinweber, V. T., Klingelhoefer, F., Neben, S., Reichert, C., Aslanian, D., Matias, L., et al. (2013). The crustal structure of the Central Mozambique continental margin - Wide-angle seismic, gravity and magnetic study in the Mozambique Channel, Eastern Africa. *Tectonophysics*, *599*, 170–196. https://doi.org/10.1016/j.tecto.2013.04.015

Leprêtre, A., Schnürle, P., Evain, M., Verrier, F., Moorcroft, D., De Clarens, P., et al. (2021). Deep structure of the North Natal Valley (Mozambique) using combined wide-angle and reflection seismic data. *Journal of Geophysical Research: Solid Earth*, *126*, e2020JB021171. https://doi.org/10.1029/2020JB021171

Leroy, S., Lucazeau, F., d'Acremont, E., Watremez, L., Autin, J., Rouzo, S., et al. (2010). Contrasted styles of rifting in the eastern Gulf of Aden: A combined wide-angle MCS and Heat flow survey. *Geochemistry, Geophysics, Geosystems*, *11*, Q07004. https://doi.org/10.1029/2009GC002963

Li, H., Tang, Y., Moulin, M., Aslanian, D., Evain, M., Schnurle, P., et al. (2021). Seismic evidence for crustal architecture and stratigraphy of the Limpopo Corridor: New insights into the evolution of the sheared margin offshore southern Mozambique. *Marine Geology*, *435*, 106468. https://doi.org/10.1016/j.margeo.2021.106468

Loncke, L., Roest, W. R., Klingelhoefer, F., Basile, C., Graindorge, D., Heuret, A., & de Lépinay, M. M. (2019). Transform marsginal plateaus. *Earth-Science Reviews*. https://doi.org/10.1016/j.earscirev.2019.102940

Lorenzo, J. M. (1997). Sheared continent–ocean margins: An overview. *Geo-Marine Letters*, *17*(1), 1–3. https://doi.org/10.1007/PL00007201

Lorenzo, J. M., & Wessel, P. (1997). Flexure across a continent–ocean fracture zone: The northern Falkland/Malvinas Plateau, South Atlantic. *Geo-Marine Letters*, *17*(1), 110–118. https://doi.org/10.1007/s003670050015

Lucazeau, F., Leroy, S., Rolandone, F., d'Acremont, E., Watremez, L., Bonneville, A., et al. (2010). Heat-flow and hydrothermal circulation at the ocean–continent transition of the eastern gulf of Aden. *Earth and Planetary Science Letters*, *295*(3–4), 554–570. https://doi.org/10.1016/j.epsl.2010.04.039

Macgregor, D. (2018). History of the development of Permian–Cretaceous rifts in East Africa: A series of interpreted maps through time. *Petroleum Geoscience*, *24*(1), 8–20. https://doi.org/10.1144/petgeo2016-155

Mahanjane, E. S. (2014). The Davie Fracture Zone and adjacent basins in the offshore Mozambique Margin–A new insights for the hydrocarbon potential. *Marine and Petroleum Geology*, *57*, 561–571. https://doi.org/10.1016/j.marpetgeo.2014.06.015

Mahanjane, S. E. (2012). A geotectonic history of the northern Mozambique Basin including the Beira High - A contribution for the understanding of its development. *Marine and Petroleum Geology*, *36*, 1–12. https://doi.org/10.1016/j.marpetgeo.2012.05.007

Manatschal, G. (2004). New models for evolution of magma-poor rifted margins based on a review of data and concepts from West Iberia and the Alps. *International Journal of Earth Sciences*, *93*(3), 432–466. https://doi.org/10.1007/s00531-004-0394-7

Mascle, J. (1976). Atlantic-type continental margins: Distinction of two basic structural types. *An. Acad. Bras. Cienc*, *48*, 191–197.

Mascle, J., & Blarez, E. (1987). Evidence for transform margin evolution from the Ivory Coast–Ghana continental margin. *Nature*, *326*(6111), 378–381. https://doi.org/10.1038/326378a0

Melluso, L., Cucciniello, C., Petrone, C. M., Lustrino, M., Morra, V., Tiepolo, M., & Vasconcelos, L. (2008). Petrology of Karoo volcanic rocks in the southern Lebombo monocline, Mozambique. *Journal of African Earth Sciences*, *52*(4–5), 139–151. https://doi.org/10.1016/j.jafrearsci.2008.06.002

Mercier de Lépinay, M., Loncke, L., Basile, C., Roest, W. R., Patriat, M., Maillard, A., & de Clarens, P. (2016). Transform continental margins - Part 2: A worldwide review. *Tectonophysics*, *693*, 96–115. https://doi.org/10.1016/j.tecto.2016.05.038

Momoh, E., Cannat, M., & Leroy, S. (2020). Internal structure of the oceanic lithosphere at a melt-starved ultra-slow-spreading mid-ocean ridge: Insights from 2-D seismic data. *Geochemistry, Geophysics, Geosystems*, *21*, e2019GC008540. https://doi.org/10.1029/2019GC008540

Momoh, E., Cannat, M., Watremez, L., Leroy, S., & Singh, S. C. (2017). Quasi-3-D Seismic Reflection Imaging and Wide-Angle Velocity Structure of Nearly Amagmatic Oceanic Lithosphere at the Ultraslow-Spreading Southwest Indian Ridge. *Journal of Geophysical Research: Solid Earth*, *122*(12), 9511–9533. https://doi.org/10.1002/2017JB014754

Mougenot, D., Gennesseaux, M., Hernandez, J., Lepvrier, C., & Malod, J. A. (1991). La ride du Mozambique (Océan Indien): Un fragment continental individualise lors du coulissement de l'Amérique et de l'Antarctique le long de l'Afrique de l'Est? *Comptes rendus de l'Académie des sciences. Série 2, Mécanique, Physique, Chimie, Sciences de l'univers, Sciences de la Terre*, *312*(6), 655–662.

Moulin, M., & Aslanian, D. (2016). *PAMELA-MOZ03 cruise, RV Pourquoi pas?* https://doi.org/10.17600/16001600

Moulin, M., Aslanian, D., Evain, M., Leprêtre, A., Schnurle, P., Verrier, F., et al. (2020). Gondwana breakup: Messages from the North Natal Valley. *Terra Nova*, *32*, 205–214. https://doi.org/10.1111/ter.12448

Moulin, M., & Evain, M. (2016). *PAMELA-MOZ05 cruise, RV Pourquoi pas?* https://doi.org/10.17600/16009500

Mueller, C. O., & Jokat, W. (2017). Geophysical evidence for the crustal variation and distribution of magmatism along the central coast of Mozambique. *Tectonophysics*, *712–713*, 1–703. https://doi.org/10.1016/j.tecto.2017.06.007

Mueller, C. O., & Jokat, W. (2019). The initial Gondwana break-up - A synthesis based on new potential field data of the Africa-Antarctica Corridor. *Tectonophysics*, *750*, 301–328. https://doi.org/10.1016/j.tecto.2018.11.008

Mutter, J. C., & Carton, H. D. (2013). The Mohorovicic discontinuity in ocean basins: Some observations from seismic data. *Tectonophysics*, *609*, 314–330. https://doi.org/10.1016/j.tecto.2013.02.018

Nemčok, M., Rybár, S., Sinha, S. T., Hermeston, S. A., & Ledvényiová, L. (2016). Transform margins: Development, controls and petroleum systems–an introduction. *Geological Society, London, Special Publications*, *431*(1), 1–38. https://doi.org/10.1144/SU431.15

Nguyen, L. C., Hall, S. A., Bird, D. E., & Ball, P. J. (2016). Reconstruction of the East Africa and Antarctica continental margins. *Journal of Geophysical Research - Solid Earth*, *121*, 4156–4179. https://doi.org/10.1002/2015JB012776

Nyblade, A. A., & Robinson, S. W. (1994). The african superswell. *Geophysical Research Letters*, *21*(9), 765–768. https://doi.org/10.1029/94GL00631

Planke, S., Symonds, P. A., Alvestad, E., & Skogseid, J. (2000). Seismic volcanostratigraphy of large-volume basaltic extrusive complexes on rifted margins. *Journal of Geophysical Research: Solid Earth*, *105*(B8), 19335–19351. https://doi.org/10.1029/1999JB900005

Ponte, J.-P., Robin, C., Guillocheau, F., Popescu, S., Suc, J.-P., Dall'Asta, M., et al. (2019). The Zambezi delta (Mozambique channel, East Africa): High resolution dating combining bio-orbital and seismic stratigraphy to determine climate (palaeoprecipitation) and tectonic controls on a passive margin. *Marine and Petroleum Geology*, *105*, 293–312. https://doi.org/10.1016/j.marpetgeo.2018.07.017

Raillard, S. (1990). *Les marges de lAfrique de lEst et les zones de fracture associees: Chaine Davie et Ridge du Mozambique-Champagne MD-60/MACA MO-11 (Doctoral dissertation, PhD dissertation*. Universite Pierre et Marie Curie.

Reeves, C. V. (2017). The development of the East African margin during Jurassic and Lower Cretaceous times: A perspective from global tectonics. *Petroleum Geoscience*, *24*(1), 41–56. https://doi.org/10.1144/petgeo2017-021

Reeves, C. V., Teasdale, J. P., & Mahanjane, E. S. (2016). Insight into the Eastern Margin of Africa from a new tectonic model of the Indian Ocean. In M. Nemčok, S. Rybár, S. T. Sinha, S. A. Hermeston, & L. Ledvényiová (Eds.), *Transform margins: Development, controls and petroleum systems* (Vol. 431, pp. 299–322). Geological Society, London, Special Publications. https://doi.org/10.1144/sp431.12

Riley, T. R., Millar, I. L., Watkeys, M. K., Curtis, M. L., Leat, P. T., Klausen, M. B., & Fanning, C. M. (2004). U–Pb zircon (SHRIMP) ages for the Lebombo rhyolites, South Africa: Refining the duration of Karoo volcanism. *Journal of the Geological Society*, *161*(4), 547–550. https://doi.org/10.1144/0016-764903-181

Ring, U., Kröner, A., Buchwaldt, R., Toulkeridis, T., & Layer, P. W. (2002). Shear-zone patterns and eclogite-facies metamorphism in the Mozambique belt of northern Malawi, East-Central Africa: Implications for the assembly of Gondwana. *Precambrian Research*, *116*(1–2), 19–56. https://doi.org/10.1016/S0301-9268(01)00233-9

Roddick, J. C., Cliff, R. A., & Rex, D. C. (1980). The evolution of excess argon in Alpine biotites—a40Ar-39Ar analysis. *Earth and Planetary Science Letters*, *48*(1), 185–208. https://doi.org/10.1016/0012-821X(80)90181-8

Sage, F., Basile, C., Mascle, J., Pontoise, B., & Whitmarsh, R. B. (2000). Crustal structure of the continent–ocean transition off the Cote d'Ivoire–Ghana transform margin: Implications for thermal exchanges across the palaeotransform boundary. *Geophysical Journal International*, *143*(3), 662–678. https://doi.org/10.1046/j.1365-246X.2000.00276.x

Saggerson, E. P., & Bristow, J. W. (1983). The geology and structural relationships of the southern Lebombo volcanic and intrusive rocks, South Africa. *Bulletin of Volcanology*, *46*, 161–181. https://doi.org/10.1007/bf02597583

Salman, G., & Abdula, I. (1995). Development of the Mozambique and Ruvuma sedimentary basins, offshore Mozambique. *Sedimentary Geology*, *96*(1–2), 7–41. https://doi.org/10.1016/0037-0738(95)00125-R

Sauter, D., Werner, P., Ceuleneer, G., Manatschal, G., Rospabé, M., Tugend, J., et al. (2021). Sub-axial deformation in oceanic lower crust: Insights from seismic reflection profiles in the Enderby Basin and comparison with the Oman ophiolite. *Earth and Planetary Science Letters*, *554*, 116698. https://doi.org/10.1016/j.epsl.2020.116698

Scrutton, R. A. (1979). Structure of the crust and upper mantle at Goban Spur, southwest of the British Isles—Some implications for margin studies. *Tectonophysics*, *59*(1–4), 201–215. https://doi.org/10.1016/0040-1951(79)90045-3

Segoufin, J., & Patriat, P. (1981). Reconstructions de l'Ocean Indien Occidental pour les epoques des anomalies M21, M2 et 34; Paleoposition de Madagascar. *Bulletin de la Societe Geologique de France*, *7*(6), 603–607. https://doi.org/10.2113/gssgfbull.S7-XXIII.6.603

Şengör, A. M. C. (2001). Elevation as indicator of mantleplume activity. In R. E. Ernst, & K. L. Buchan (Eds.), *Mantle plumes: Their identification through time* (Vol. 352, pp. 183–225). Geological Society of America Special Paper. https://doi.org/10.1130/0813723523.183

Senkans, A., Leroy, S., d'Acremont, E., Castilla, R., & Despinois, F. (2019). Polyphase rifting and break-up of the central Mozambique margin. *Marine and Petroleum Geology*, *100*, 412–433. https://doi.org/10.1016/j.marpetgeo.2018.10.035

Seton, M., Müller, R. D., Zahirovic, S., Gaina, C., Torsvik, T., Shephard, G., et al. (2012). Global continental and ocean basin reconstructions since 200 Ma. *Earth-Science Reviews*, *113*(3–4), 212–270. https://doi.org/10.1016/j.earscirev.2012.03.002

Skogseid, J., Pedersen, T., Eldholm, O., & Larsen, B. T. (1992). Tectonism and magmatism during NE Atlantic continental break-up: The Vøring Margin. *Geological Society, London, Special Publications*, *68*(1), 305–320. https://doi.org/10.1144/GSL.SP.1992.068.01.19

Storey, B. C., & Kyle, P. R. (1997). An active mantle mechanism for Gondwana breakup. *South African Journal of Geology*, *100*(4), 283–290.

Svensen, H., Corfu, F., Polteau, S., Hammer, Ø., & Planke, S. (2012). Rapid magma emplacement in the Karoo large igneous province. *Earth and Planetary Science Letters*, *325*, 1–9. https://doi.org/10.1016/j.epsl.2012.01.015

Thompson, J. O., Moulin, M., Aslanian, D., De Clarens, P., & Guillocheau, F. (2019). New starting point for the Indian Ocean: Second phase of breakup for Gondwana. *Earth-Science Reviews*, *191*, 26–56. https://doi.org/10.1016/j.earscirev.2019.01.018

Tremblay, A., Ruffet, G., & Lemarchand, J. (2020). *Timing and duration of Archean orogenic gold deposits in the Bourlamaque pluton, Val d'Or mining camp, Abitibi, Canada* (Vol. 127, p. 103812). Ore Geology Reviews. https://doi.org/10.1016/j.oregeorev.2020.103812

Tucholke, B. E., Houtz, R. E., & Barrett, D. M. (1981). Continental crust beneath the Agulhas plateau, southwest Indian Ocean. *Journal of Geophysical Research*, *86*(B5), 3791–3806. https://doi.org/10.1029/JB086iB05p03791

Turner, G. (1971). 40Ar39Ar ages from the lunar maria. *Earth and Planetary Science Letters*, *11*(1–5), 169–191. https://doi.org/10.1016/0012-821X(71)90161-0

Watkeys, M. K. (2002). *Development of the Lebombo rifted volcanic margin of southeast Africa* (pp. 27–46). Special Papers-Geological Society of America. https://doi.org/10.1130/0-8137-2362-0.27

Watkeys, M. K., & Sokoutis, D. (1998). Transtension in southeastern Africa associated with Gondwana break-up. *Geological Society, London, Special Publications*, *135*(1), 203–214. https://doi.org/10.1144/GSL.SP.1998.135.01.13

Watremez, L., Leroy, S., d'Acremont, E., Roche, V., Evain, M., Leprêtre, A., et al. (2021). The Limpopo magma-rich transform margin, South Mozambique – Part 1: Insights from deep-structure seismic imaging. *Tectonics*. https://doi.org/10.1029/2021tc006915

White, R., & McKenzie, D. (1989). Magmatism at rift zones: The generation of volcanic continental margins and flood basalts. *Journal of Geophysical Research*, *94*(B6), 7685–7729. https://doi.org/10.1029/JB094iB06p07685

White, R. S. (1997). Mantle plume origin for the Karoo and Ventersdorp flood basalts, South Africa. *South African Journal of Geology*, *100*(4), 271–282.

Woolley, A. R. (1991). The Chilwa Alkaline Igneous Province of Malawi: A Review. In A. B. Kampunzu, & R. T. Lubala (Eds.), *Magmatism in extensional structural settings* (pp. 377–409). Springer. https://doi.org/10.1007/978-3-642-73966-8_15